



**Faculty of Graduated Studies**

**Copper(II) complexes of Anti-inflammatory drugs with Nitrogen  
Based Ligands: Synthesis, Characterization and Biological Activities**

مركبات النحاس ثنائي الشحنة مع أدوية ضد الالتهابات و بعض القواعد النيتروجينية: تحضير، تشخيص  
و دراسة للفعاليات الحيوية

**This Thesis is Submitted in Partial Fulfilment of the Requirements for the  
Degree of Master in Applied Chemistry from the Faculty of Graduate Studies at  
Birzeit University, Birzeit, Palestine.**

**By**

**Mutasem Ibrahim Naser aldeen**

\*\*\*\*\*

**Under Supervision of**

**Dr. Abdul Latif Abu Hijleh**

**June/2014**

**MASTER'S EXAMINATION COMMITTEE:**

---

Dr. Abdul Latif Abu Hijleh

---

Date

Department of Chemistry, Birzeit University

Supervisor

---

Dr. Hijazi Abu Ali

---

Date

Department of Chemistry, Birzeit University

Member

---

Dr. Mazen Hamed

---

Date

Department of Chemistry, Birzeit University

Member

## **ACKNOWLEDGMENTS**

I would like to express my gratitude to my supervisor Dr. Abdul Latif Abu Hijleh for giving me the opportunity to work with him and under his supervision, support and patience provided throughout my thesis.

I would also thank other members of the thesis committee, Dr. Hijazi Abu Ali and Dr. Mazen Hamed for their recommendations and insightful comments.

I am very grateful to the staff and my colleagues in the Chemistry Department Ibrahim shalash, Ahmad Amer, Assem Mubarak, Mohanad Darweesh, Muath Nairat, Sadieh abu sirriah, and Salam Maloul for their encouragement, friendship and support.

Finally, I would like to thank my parents for their endless support, patience and encouragement throughout the course of my studies.

Birzeit, June, 2014

Mutasem Naser Aldeen

## TABLE OF CONTENTS

Acknowledgments .....	I
Table of contents.....	II
List of figures.....	V
List of tables.....	VII
List of schemes .....	VIII
List of abbreviations .....	IX
Abstract.....	XI
المُلخَص بالعربية (Arabic abstract).....	XII
<b>1 INTRODUCTION .....</b>	<b>1</b>
1.1. General introduction.....	1
1.2. General copper chemistry.....	2
1.2.1. Oxidation states of copper .....	3
1.3. Coordination chemistry of copper.....	4
1.3.1. Metal carboxylates.....	5
1.3.2. Copper carboxylate complexes.....	7
1.3.3. Copper complexes with non-steroidal anti-inflammatory drugs (NSAIDs) .....	8
1.4. Copper complexes with nitrogen donor heterocyclic ligand.....	10
1.5. Copper containing metalloproteins .....	11
1.5.1. Types of copper enzymes .....	13
1.6. Catalytic activities of copper complexes.....	15
1.6.1. Catechol oxidase (CO).....	15

1.6.2. Phenoxazinone synthase .....	16
1.6.3. Oxidation of <i>o</i> -phenylenediamine .....	17
1.7. The aim of the present work.....	18
<b>2. EXPERIMENTAL SECTION .....</b>	<b>19</b>
2.1. Reagents and materials .....	19
2.2. Physical measurements .....	19
2.3. Synthesis of copper(II) complexes.....	20
2.3.1. Synthesis of [Cu(sal) <sub>2</sub> (pz) <sub>2</sub> ] ( <b>1</b> ).....	20
2.3.2. Synthesis of [Cu(nap) <sub>2</sub> (pz) <sub>4</sub> ] ( <b>2</b> ) .....	21
2.3.3. Synthesis of [Cu <sub>2</sub> (nap) <sub>4</sub> (mtd) <sub>2</sub> ] ( <b>3</b> ).....	21
2.4. X-ray crystallography.....	22
2.5. Biological activity studies .....	25
2.5.1. Catechol oxidase activity .....	25
2.5.2. Solvent-dependent catecholase activity .....	26
2.5.3. Phenoxazinone synthase activity .....	26
2.5.4. Oxidation of <i>o</i> -phenylenediamine activity.....	27
<b>3. RESULTS AND DISCUSSIONS.....</b>	<b>28</b>
3.1. Synthesis of complexes .....	28
3.2. Magnetic and spectroscopic results.....	31
3.3. Crystal structure of complexes .....	35
3.3.1. Crystal structure of complex 1 .....	35

3.3.2. Crystal structure of complex 2 .....	37
3.4. Biological activity studies .....	39
3.4.1. Catechol oxidase activity .....	39
3.4.2. Solvent-dependent catecholase activity .....	45
3.4.3. Phenoxazinone synthase activity.....	47
3.4.4. Oxidation of <i>o</i> -phenylenediamine (OPD) to 2,3-diaminophenazine (DAP) .....	52
4. REFERENCES .....	57
5. APPENDICES .....	61
APPENDIX A: Structure of [Cu(sal) <sub>2</sub> (pz) <sub>2</sub> ] ( <b>1</b> ). .....	61
APPENDIX B: Structure of [Cu(nap) <sub>2</sub> (pz) <sub>4</sub> ] ( <b>2</b> ). .....	68

## LIST OF FIGURES

<b>Figure 1.1</b> Metal-Carboxylate binding modes.....	6
<b>Figure 1.2</b> Different structures of copper(II) carboxylates: mononuclear and dinuclear copper carboxylate.....	7
<b>Figure 1.3</b> (A): Structure of salicylic acid, (B-E): some of the possible coordination modes of salicylic acid. ....	9
<b>Figure 1.4</b> Some nitrogen donor heterocyclic ligands that can coordinate to copper(II) ion.....	11
<b>Figure 1.5</b> Some copper containing metalloprotein active sites.....	12
<b>Figure 3.1</b> Structure of $[\text{Cu}(\text{sal})_2(\text{pz})_2]$ , ( <b>1</b> ). ....	36
<b>Figure 3.2</b> Structure of $[\text{Cu}(\text{nap})_2(\text{pz})_4]$ , ( <b>2</b> ). ....	38
<b>Figure 3.3</b> Oxidation of 3,5-dtbc by <b>1</b> monitored by Uv-Vis spectroscopy and the increase in absorption at 400 nm with time .....	40
<b>Figure 3.4</b> The increase in absorption at 400 nm with time of 3,5-DTBC that treated with various complex <b>1</b> concentrations (left). First-order plot for $\ln$ Rate ( $\text{s}^{-1}$ ) verses $\ln$ [complex <b>1</b> ] (right).....	44
<b>Figure 3.5</b> The increase in absorption at 400 nm with time of complex <b>1</b> that treated with various [3,5-dtbc] (left). Plot for initial rate ( $\text{s}^{-1}$ ) verses [complex <b>1</b> ] (right).....	45
<b>Figure 3.6</b> Oxidation of 3,5-dtbc by <b>3</b> monitored by Uv-Vis spectroscopy at 400 nm in: ( <b>I</b> ) methanol, ( <b>II</b> ) in dichloromethane, ( <b>III</b> ) in acetonitrile.....	46
<b>Figure 3.7</b> The oxidation of 3,5-DTBC with complex <b>1</b> ( <b>I</b> ), complex <b>2</b> ( <b>II</b> ), and complex <b>3</b> ( <b>III</b> ) in different solvents.....	47
<b>Figure 3.8</b> Oxidation of OAP by <b>2</b> (left). The increase in absorption at 430 nm with time (right).....	48

- Figure 3.9** The increase in absorption at 430 nm with time of OAP that treated with various [complex **3**] (left). First-order plot for  $\ln \text{Rate (s}^{-1}\text{)}$  verses  $\ln$  [complex **3**] (right) .....50
- Figure 3.10** The increase in absorption at 430 nm with time of complex **3** that treated with various [OAP] (left). Plot for initial rate ( $\text{s}^{-1}$ ) verses [complex **3**] (right). .....51
- Figure 3.11** Oxidation reaction of OPD by **3** .....53
- Figure 3.12** The increase in absorption at 430 nm with time of OPD that treated with various [complex **1**] (left). First-order plot for  $\ln \text{Rate (s}^{-1}\text{)}$  verses  $\ln$  [complex **1**] (right) .....54
- Figure 3.13** The increase in absorption at 430 nm with time of complex **1** that treated with various [OPD] (left). Plot for initial rate ( $\text{s}^{-1}$ ) verses [complex **3**] (right). .....55



## LIST OF TABLES

<b>Table 1.1</b> Some of essential metal-containing biomolecules, examples and their role in biological system.....	1
<b>Table 1.2</b> Redox chemistry of copper ions in aqueous solution.....	3
<b>Table 1.3</b> Selected copper containing protein/enzyme active sites, biological functions, and catalysed reactions.....	13
<b>Table 1.4</b> Type I, II, and III of biological copper sites in most copper proteins, geometry, and chemical structure for specific examples.....	14
<b>Table 2.1</b> Data and structure refinement for <b>1</b> and <b>2</b> .....	24
<b>Table 2.2</b> Selected bond lengths (Å) and bond angles (°) for complex <b>1</b> .....	24
<b>Table 2.3</b> Selected bond lengths (Å) and bond angles (°) for complex <b>2</b> .....	25
<b>Table 3.1</b> Magnetic and spectral data for the complexes <b>1-3</b> .....	33
<b>Table 3.2</b> Hydrogen bonds for complex <b>1</b> [Å and °]......	37
<b>Table 3.3</b> Hydrogen bonds for complex <b>2</b> [Å and °]......	39
<b>Table 3.4</b> Copper complexes activity for the aerobic oxidation of 3,5-dtbc.....	41
<b>Table 3.5</b> Order of the reaction with respect to complex for the oxidation reaction of 3,5-DTBC, OPD, and OAP substrates by complexes <b>1-3</b> .....	44
<b>Table 3.6</b> Initial rates for the oxidation of 3,5-DTBC in MeOH, CH <sub>2</sub> Cl <sub>2</sub> and acetonitrile by complexes <b>1-3</b> .....	47
<b>Table 3.7</b> Copper complexes activity for the aerobic oxidation of <i>o</i> -aminophenol ..	49
<b>Table 3.8</b> Copper complexes activity for the aerobic oxidation of OPD.....	53

## LIST OF SCHEMES

<b>Scheme 1.1</b> Conversion of catechol to corresponding <i>o</i> -quinone .....	16
<b>Scheme 1.2</b> Overall equation of the oxidation of <i>o</i> -aminophenol (OAP) to 2-amino-3H-phenoxazin-3-one using copper complexes as a catalyst.....	16
<b>Scheme 1.3</b> Oxidation of OPD to DAP using Horseradish peroxidase or hemoglobin as a catalyst.....	17
<b>Scheme 3.1</b> The general synthesis of complex <b>1</b> at room temperature.....	29
<b>Scheme 3.2</b> The general synthesis of complex <b>2</b> and <b>3</b> at room temperature.....	30
<b>Scheme 3.3</b> Proposed mechanism for the oxidation of catechol by dicopper(II) complexes.....	42
<b>Scheme 3.4</b> Proposed mechanism for the oxidation of catechol by mononuclear copper(II) complexes.....	43
<b>Scheme 3.5</b> Proposed reaction mechanism for formation of APX from OAP catalysed by copper(II) complexes. ....	52
<b>Scheme 3.6</b> Proposed reaction mechanism for the formation of DAP from OPD catalysed by copper(II) complexes .....	56

## LIST OF ABBREVIATIONS

NSAIDs	Non-steroidal anti-inflammatory drugs
Nap	Naproxen
Pz	Pyrazole
Mtnd	Metronidazole
Sal	Salicylate
3,5-DTBC	3,5-Di-tert-butylcatechol
3,5-DTBQ	3,5-Di-tert-butyl- <i>o</i> -benzoquinone
OPD	<i>o</i> -Phenylenediamine
DAP	2,3-Diaminophenazine
OAP	<i>o</i> -Aminophenol
APX	2-Amino-3 <i>H</i> -phenoxazine-3-one
min	Minute(s)
s	Second
ml	Milli; Litter(s)
mol	Mole(s)
μ	Micro
IR	Infrared spectroscopy
ε	Extension coefficient
Uv-Vis	Ultraviolet-Visible
m.p	Melting point
MeOH	Methanol

DCM	Dichloromethane
Asp	Aspartic acid
His	Histadine
Tyr	Tyrosine
Cys	Cystine

## Abstract

Copper(II) complexes of two non-steroidal anti-inflammatory drugs (NSAIDs) naproxen (nap) and salicylate (sal) with nitrogen donor ligands pyrazole (pz) and metronidazole (mtnd), [Cu(sal)<sub>2</sub>(pz)<sub>2</sub>] (**1**), [Cu(nap)<sub>2</sub>(pz)<sub>4</sub>] (**2**), [Cu<sub>2</sub>(nap)<sub>4</sub>(mtnd)<sub>2</sub>] (**3**) have been synthesized and spectroscopically characterized. The crystal structure of complex (**1**) and (**2**) has been determined by X-ray crystallography. In complex **1** the Cu(II) ion is coordinated with two nitrogen of pyrazoles and two oxygens of the salicylate carboxylate groups in copper atom plan and with the other two oxygen atoms of the carboxylate groups at longer distances in the axial sites to yield *trans*-CuN<sub>2</sub>O<sub>2</sub> + O<sub>2</sub> chromophore. In complex **2** Cu(II) ion is coordinated in the plan with four nitrogen of pyrazoles and the axial sites are occupied by two oxygen of the naproxenato carboxylate groups to yield CuN<sub>4</sub> + O<sub>2</sub> chromophore. The catalytic oxidase activities of complexes toward the aerobic oxidations of 3,5-di-tert-butylcatechol (3,5-DTBC) to 3,5-di-tert-butyl-*o*-benzoquinone (3,5-DTBQ), *o*-phenylenediamine (OPD) to 2,3-diaminophenazine (DAP), and *o*-aminophenol (OAP) to 2-amino-3H-phenoxazine-3-one (APX) have been studied. Solvents-dependent catecholase activity of these complexes solvents: methanol (MeOH), dichloromethane (DCM), and acetonitrile (ACN) also have been studied. The catalytic activities of these complexes mimic those of copper-containing enzymes catecholase and phenoxazinone synthase.

## الملخص بالعربية

هذا البحث قائم على تحضير، تشخيص، ودراسة الأنشطة الحيوية لمركبات أيون النحاس ثنائي الشحنة المرتبط بالكربوكسلات المضادة للالتهابات كالنبروكسين وحامض السلسليك مع القواعد النيتروجينية البيروزول والميترونيدازول. المركبات التي تم تحضيرها في هذا البحث هي:



التركيبية البلورية للمركب (1) و (2) تمّ تحديدها بواسطة جهاز الأشعة السينية لدراسة البلورات والتي أكدت أنّ المركب الأول لديه التركيب البنائية  $\text{trans-CuN}_2\text{O}_2 + \text{O}_2$  الناتجة عن ارتباط أيون النحاس ثنائي الشحنة بذرتي أكسجين التسلسلات وذرتي نيتروجين البيروزول. المركب الثاني لديه التركيب البنائية  $\text{CuN}_4 + \text{O}_2$  الناتجة عن ارتباط أيون النحاس ثنائي الشحنة بذرتي أكسجين جاءت من النبروكسينات وأربع ذرات نيتروجين جاءت من البيروزول. كما وتمّت دراسة بعض الأنشطة الحيوية للمركبات في الظروف العادية للغرفة من خلال قدرتها على تأكسد كل من  $3,5\text{-di-tert-butylcatechol}$  (3,5-dtbc) و  $o\text{-phenylenediamine}$  (OPD) و  $o\text{-aminophenol}$  إلى  $3,5\text{-di-tert-butyl-}o\text{-benzoquinone}$  (3,5-dtbq) و  $2,3\text{-diaminophenazine}$  و  $2,3\text{-DAP}$  و  $2\text{-amino-3H-phenoxazine-3-one}$  (APX) على الترتيب، بالإضافة إلى دراسة مدى تأثير كل من المحاليل التالية:  $\text{acetonitrile}$  ،  $\text{dichloromethane}$  ،  $\text{methanol}$  على تأكسد (3,5-dtbc) إلى (3,5-dtbq). إنّ دراسة الأنشطة الحيوية لهذه المركبات أثبتت أنّ لها القدرة على محاكاة الأنزيمات التي تحتوي على ذرة النحاس مثل  $\text{catecholase}$  و  $\text{phenoxazinone synthase}$ .

# 1 INTRODUCTION

## 1.1.General introduction

Metals are spread all over Earth's crust as components of important natural sources such as water, lands, and within living organisms. Approximately one-third of all known proteins that include metals such as iron, zinc and copper as cofactor(s) play a vital role in biological process as activation of dioxygen, protein structure stabilization, enzyme catalysis and critical reactions (**Table 1.1**).<sup>1,2,3</sup>

**Table 1.1** Some of essential metal-containing biomolecules, examples and their role in biological system<sup>4</sup>

Category	Biological function	Examples (metal ion involved)
Nonproteins	metal transport and structural	siderophores (Fe); skeletal (Ca, Si)
Proteins	photo-redox oxygen transport structural	chlorophyll (Mg) hemocyanin (Cu) Zn fingers (Zn)
Enzymes	electron transfer oxidation of phenol oxido – reductases	cytochromes (Fe); azurin (Cu) catechole oxidase (Cu) phenoxazinone synthase (Cu); nitrogenases (Fe, Mo, V)
	isomerases and synthesases	vitamin B12 coenzymes (Co)

On the other hand, there are less than half of the known metals have the potential for toxicity to humans and animals<sup>5</sup> and some of metals have been confirmed as carcinogens in experimental studies on animals such as Ni, Cr, As, Cd and Be.<sup>6</sup>

## 1.2. General copper chemistry

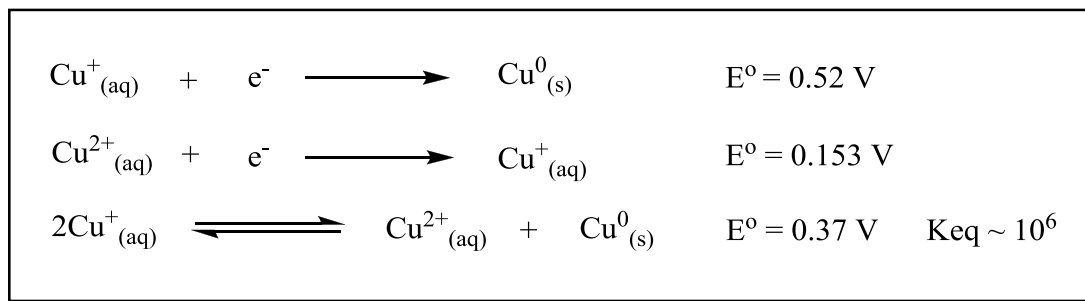
Copper (Cu) is one of essential elements for life that can be classified as a trace element.<sup>7</sup> It's also known as the third most abundant transition metal found in biology, after iron and zinc.<sup>8</sup> More than 30 enzymes containing copper ions as cofactor in human and animals for maintaining cellular activities, potential synergetic activity with drugs and other specific function such as metabolism.<sup>9,10</sup> The typical concentration of copper ion is 50 ppm in earth's crust, and 1.0 ppm in human blood.<sup>4</sup> Increasing attention has been paid to medicinal chemistry of copper because the high-affinity of the major biological fluid in human (blood plasma) to bind with copper, and the contribution of ceruloplasmin and albumin is more than 77% of the total copper content binding.<sup>11,12</sup> Copper deficiency causes some diseases such as severe neurological impairment,<sup>13</sup> Parkinson diseases,<sup>14</sup> Anemia,<sup>15</sup> Cardiovascular disease, Diabetes,<sup>16</sup> Menkes' disease,<sup>10</sup> and others.<sup>17</sup> On the other hand, high concentrations of copper can cause toxicity, and specific diseases such as Oxidative-Stress-Related Disorders, Wilson's diseases,<sup>18</sup> Alzheimer's disease (AD) and Atherosclerosis during aging.<sup>17</sup>



### 1.2.1. Oxidation states of copper

Copper element which is the focus of this research is a transition metal in group 11 of the periodic table with an electron configuration  $[\text{Ar}]4s^13d^{10}$  in the zero oxidation state. Four different oxidation states of copper can easily access Cu(I), Cu(II), Cu(III), and Cu(IV) described in the literature.<sup>19,20,21</sup> Cu(I) complexes are diamagnetic, unstable in aqueous solution with respects to solvation energy, and higher formation constant  $\sim 10^6$ , so Cu(I) is readily disproportionated to  $\text{Cu}_{(s)}$  and Cu(II) according to reactions in **Table 1.2**.<sup>7,8</sup>

**Table 1.2** Redox chemistry of copper ions in aqueous solution.



There is no d-d transitions for Cu(I) and the color of Cu(I) complexes is a result of charge transfer. The most stable Cu(II) complexes with coordination numbers 4,5 and 6 in a distorted geometries which are due to Jahn-Teller effect. The colors of these complexes are due to d-d transitions. Both Cu(I) and Cu(II) ions play an important role in biological system such as activation of dioxygen molecule ( $\text{O}_2$ ), Superoxide dismutase, and oxidase activities. The uncommon Cu(III) complexes

have  $d^8$  electronic configuration as in Ni(II).<sup>19,22</sup> These rare complexes can be stabilized by  $CF_3$  groups or by increasing the number of strong donor ligands<sup>23</sup> such as carboxylate, amide, oxime, and thiolates by chelation and by increasing the electron density at copper ion.<sup>24,25</sup>

### 1.3. Coordination chemistry of copper

The Coordination between copper ion and ligands can produce complexes with different stereochemistry and geometry. These complexes have been found in many diverse structures, generally present as mononuclear, binuclear and polynuclear species (**Figure 1.2**).<sup>26,27</sup> The most important and distinguishing features of copper ion are its unique chemical property that include; (1) copper ion exhibits various stereochemistry in such complexes,<sup>23,28,29</sup> (2) the extensive ability of this metal ion to bind various ligands and especially with oxygen and nitrogen donor types,<sup>30,31</sup> (3) the redox chemistry due to different oxidation states of copper ion.<sup>32</sup> Many copper complexes have been synthesized by interaction of copper(II) with biologically active ligands and found to exhibit various pharmacological effects such as antidiabetic,<sup>33</sup> antiamoebic,<sup>34</sup> anticonvulsant,<sup>35</sup> anticancer, antitumor,<sup>36</sup> anti-inflammatory,<sup>37,9</sup> antiulcer, and antimicrobial activities.<sup>38</sup>

### 1.3.1. Metal carboxylate

Carboxylate ligands ( $\text{RCOO}^-$ ) are one of the most important ligands in inorganic and bioinorganic chemistry with various physical and chemical properties depending on the nature of R group. Amino acids such as aspartates ( $\text{Asp}^-$ ), histidine (His), and cystine (Cis) are classified as one of the most biologically important carboxylate ligands in metalloprotein.<sup>39</sup> Hard soft acid base principle (HSAB) (concept of Pearson) is extremely helpful to determine the stability of metal-carboxylate complexes. According to its the fundamental role; hard acid prefer hard base and soft acid prefer soft base. Because the high affinity of hard base, such as the negatively charged oxygen of carboxylate ligands, to react with hard acid metals, a lot of stable metal-carboxylate complexes have been synthesized and characterized. The biological role of metal carboxylate complexes has been reported and displayed various activities such as anti-inflammatory and anti-cancer activities.<sup>40,41</sup> In presence of two lone pair of electrons at each oxygen of carboxylato groups the *syn-syn*, *syn-anti*, *anti-anti* binding, chelation and bridging interaction modes with metal can be achieved **Figure 1.1.**<sup>42,43,44</sup>

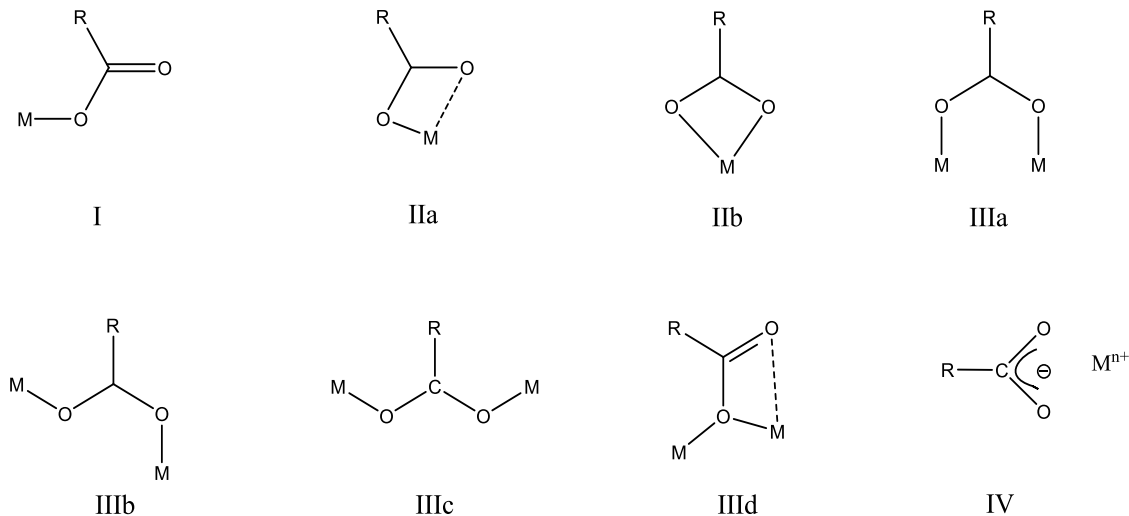


**Figure 1.1** Metal-Carboxylate binding modes: (I) monodentate,<sup>26</sup> (IIa) bidentate asymmetrical mode,<sup>45</sup> (IIb) bidentate symmetrical mode,<sup>43</sup> (IIIa) *syn-syn* mode, (IIIb) *syn-anti* mode, (IIIc) *anti-anti* mode,<sup>46</sup> (IIId) monodentate bridging,<sup>47</sup> (IV) ionic mode.

The nature of carboxylate anion binding mode to metals has been studied by Deacon and Phillips<sup>43</sup> by comparing the difference on the IR stretching frequencies between *anti*-symmetric  $\nu_{\text{asym}}(\text{COO}^-)$  and symmetric  $\nu_{\text{sym}}(\text{COO}^-)$  stretching vibrations,  $\Delta(\text{COO}^-)$ , for a great deal of metal carboxylate complexes. Based on the results of their studies the following guidelines can be used to identify the coordination mode of the carboxylate group to metal ions:  $\Delta(\text{COO}^-)$  symmetrical chelate coordination <  $\Delta(\text{COO}^-)$  ionic coordination <  $\Delta(\text{COO}^-)$  bridging coordination =  $\Delta(\text{COO}^-)$  asymmetric chelate coordination <  $\Delta(\text{COO}^-)$  monodentate coordination.<sup>42,48,49</sup>

### 1.3.2. Copper carboxylate complexes

Coordination chemistry of carboxylate groups, like those in amino acids and in other carboxylate containing ligands as in the non-steroidal anti-inflammatory drugs (NSAIDs), to copper ion is quite interesting and have been widely studied for their unique chemical properties and biological activities. A large number of mononuclear and binuclear copper(II) carboxylate complexes have been synthesized, characterized and studied their biological activities as biomimetic models for the copper containing enzymes; SOD, catechol oxidase and phenoxazinone synthase (**Figure 1.2**).<sup>49</sup>

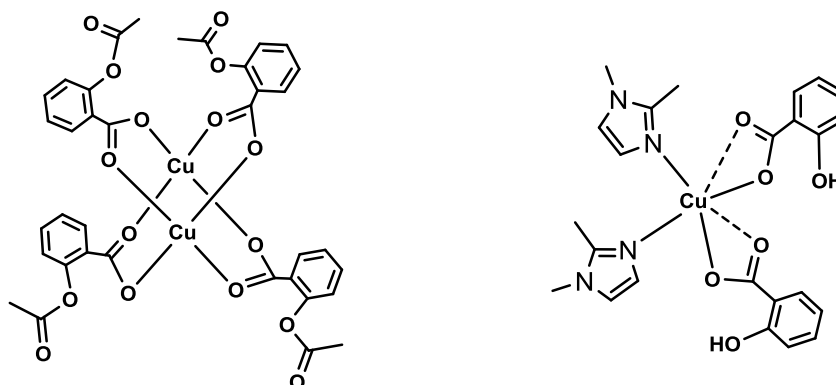


**Figure 1.2** Different structures of copper(II) carboxylates: dinuclear copper carboxylate  $[\text{Cu}_2(\text{aspirinate})_4]^{50}$  (left). mononuclear copper carboxylate  $[\text{Cu}(\text{Hsal})_2(1,2\text{-MeIm})_2]^{49}$  (right).

### **1.3.3. Copper complexes with non-steroidal anti-inflammatory drugs (NSAIDs)**

Several analgesic and antipyretic NSAIDs such as naproxen, diclofenac and salicylic acid were used as coordinated ligands to copper(II) ions (**Figure 1.2**). The interaction of copper(II) with NSAIDs enhance the activity of the drug more than the parent drug itself. In addition, the undesired side effects of the drug in humans and animals are decreased when is given as copper complex.<sup>9,49</sup> Taking into consideration the biological role and activity of copper and its complexes as well as the significance of the NSAIDs in medicine, binary and ternary of copper(II)–NSAID complexes have been synthesized and showed various biomimetic activities. For example, catechol oxidase activity toward the oxidation of phenols, superoxide dismutase mimetic activity toward scavenging the toxic superoxide anion  $O_2^{\cdot-}$  species that causes inflammation, cancer and other diseases. These biomimetic catalytic activities are important in protecting the living cell against infections and other critical diseases such as cancer and diabetes.<sup>26,49,51,52</sup>

#### **1.3.3.1. Salicylic acid**

Salicylic acid is known as 2-hydroxybenzoic acid. It became the basis for a large pharmaceutical/industrial chemistry for therapeutic treatment.<sup>9,53</sup> Salicylic acid is one of the main chemical classes of non-steroidal anti-inflammatory drug (NSAIDs), and

widely used as anti-inflammatory,<sup>9,54</sup> antifungal,<sup>55</sup> and anti-bacterial effect.<sup>56</sup> Salicylic acid has three donor oxygen; the two carboxylate oxygens and the single phenolate oxygen. Some of the possible coordination modes are shown in **Figure 1.3**.

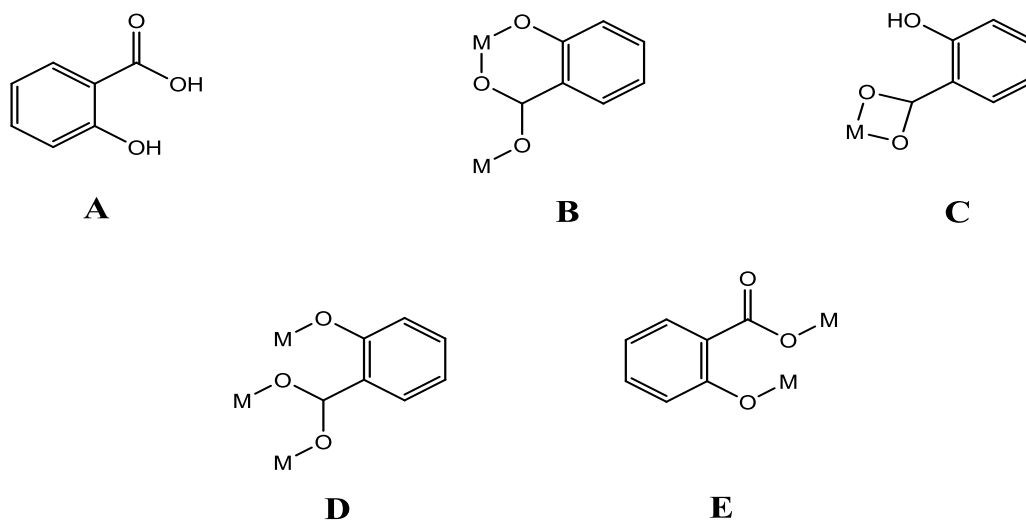


**Figure 1.3** (A): Structure of salicylic acid, (B-E): some of the possible coordination modes of salicylic acid.<sup>57</sup>

### 1.3.3.2. Naproxen

Naproxen (S)-6-Methoxy- $\alpha$ -methyl-2-naphthalenacetic acid is member of NSAIDs group of phenylalkanoic acids<sup>54</sup> with desirable biological property such as anti-inflammatory, analgesic, antipyretic.<sup>58</sup> The coordination sites of naproxen to metals can be achieved through one or two oxygen donor atoms from the carboxylate group, so three modes of coordination with metals is possible; monodentate, bidentate and

bridging (**Figure 1.1**).

#### **1.4. Copper(II) complexes with nitrogen donor heterocyclic ligand**

Coordination chemistry of nitrogen donor heterocyclic ligands such as, diimines, and imidazole derivatives such as metronidazole (**Figure 1.4**) to copper(II) is quite interesting. These ligands have been used in developing models for copper proteins/enzymes that contain natural nitrogen donor such as the essential amino acid histidine that involve imidazole functional group which coordinates with metals ions such as copper, zinc, iron and cobalt in many naturally occurring metalloproteins. Many complexes have been synthesized to understand the relationship between the coordination geometry and the redox potentials of these complexes with these nitrogen donor ligands. The histidine residue in the native enzymes has been mimicked by a model complexes that include biologically important heterocyclic nitrogen donor ligands such as imidazoles and pyrazoles which play important roles in various catalytic activities in biology.<sup>23,59,60,61,62,63</sup>



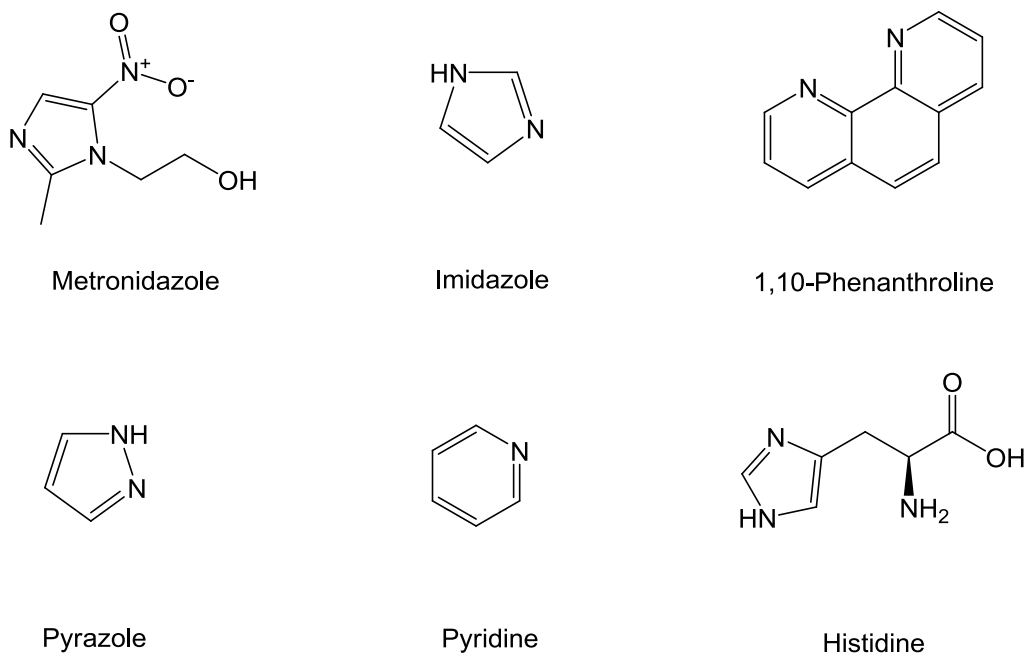


**Figure 1.4** Some nitrogen donor heterocyclic ligands that can coordinate to copper(II) ion.

### 1.5. Copper containing metalloproteins

Copper-containing metalloproteins and enzymes make copper is the third most abundant transition metal, after iron and zinc, in the human body (**Figure 1.5**).<sup>4</sup> It is an essential bio-element in biological systems,<sup>64</sup> and required for many metabolic reaction.<sup>8,65</sup> The copper ion in these proteins/enzymes is present in Cu(I) or Cu(II) oxidation state and coordinate to nitrogen, sulfur and/or oxygen donor ligands such as imidazole, cysteine, histidine and tyrosine as shown in **Figure 1.5**.<sup>7</sup>

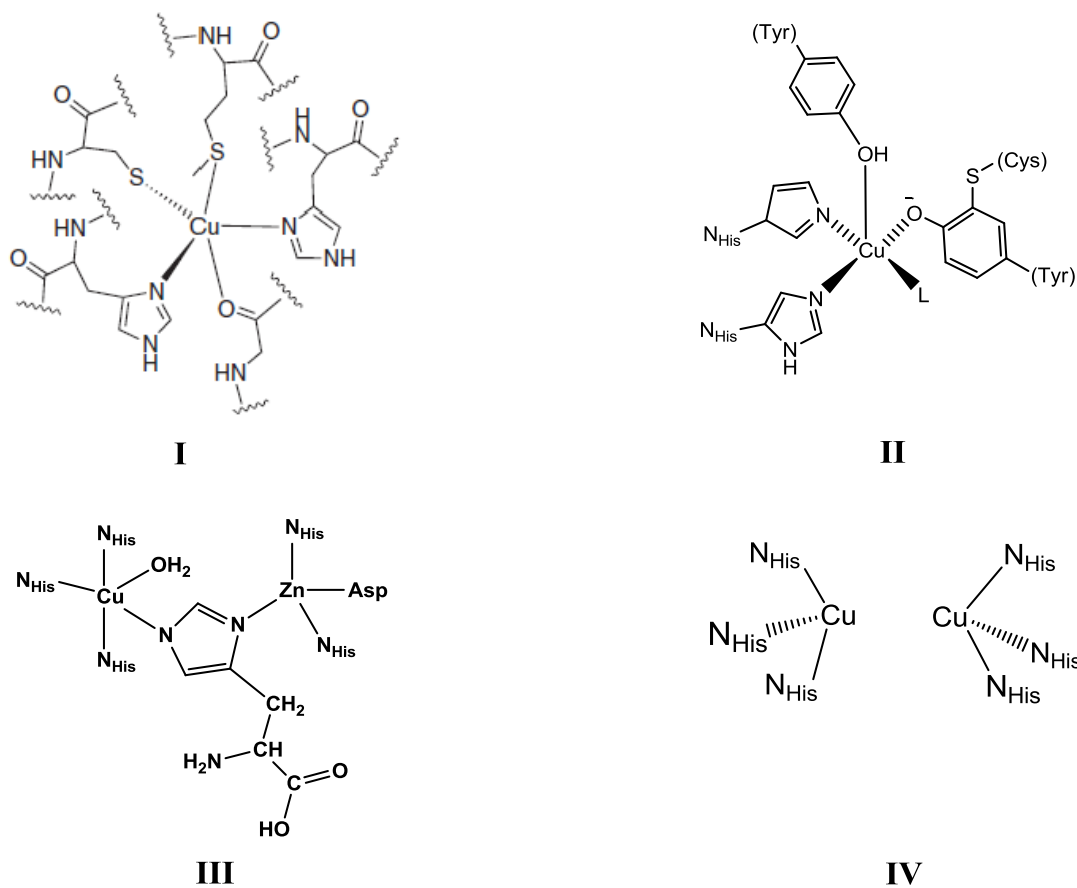


**Figure 1.5** Some copper containing metalloprotein active sites: **(I)** azurin,<sup>66</sup>  $\text{Cu}(\text{N}_{\text{His}})_2$   $\text{S}_{\text{Cys}} \text{S}_{\text{Met}} \text{O}_{\text{Gly}}$ , **(II)** galactose oxidase,<sup>67</sup> **(III)** Cu, Zn SOD in the oxidation form,<sup>68,69,70,71,72,73</sup> **(IV)** dicopper(II) center of catechol oxidase in the deoxy state.<sup>74</sup>

It's also known that copper enzymes play a major role as catalysts in oxidation reactions of different substrates such as aromatic amines and phenols, and in various biological process such as electron transport, oxygen carrier and superoxide dismutase, and many other biological activities (**Table 1.3**).

**Table 1.3** Selected copper containing protein/enzyme active sites, biological functions, and catalysed reactions.<sup>7,8,12,66,75</sup>

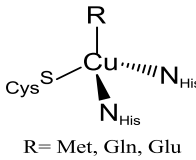
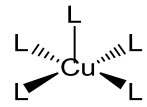
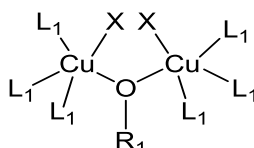
Copper protein/enzyme	Biological function	Catalyzed reaction
Plastocyanin	Electron transfer	$\text{Pc}_{(\text{ox})} + \text{e}^- \rightleftharpoons \text{Pc}_{(\text{red})}$
Azurin	Electron transfer	$\text{Az}_{(\text{ox})} + \text{e}^- \rightleftharpoons \text{Az}_{(\text{red})}$
Ascorbate oxidase	Reduction of L-ascorbate	$\text{L-Ascorbate} + \text{O}_2 \longrightarrow \text{dehydroascorbate} + \text{H}_2\text{O}$
Tyrosinase	Monophenol monooxygenase, catalyzes the oxidation of phenols, melanin synthesis	$\text{O}_2 + 2\text{H}^+ + \text{monophenol} \longrightarrow \text{o-diphenol} + \text{H}_2\text{O}$ $\text{O}_2 + 2 \text{o-diphenol} \longrightarrow 2 \text{o-quinone} + 2\text{H}_2\text{O}$
Catechol oxidase (CO)	Oxidation of <i>o</i> -catechol to <i>o</i> -quinone	$\text{o-catechol} \longrightarrow \text{o-quinone}$
Hemocyanin	O <sub>2</sub> transport	$\text{Hc} + \text{O}_2 \rightleftharpoons \text{Hc} \cdot \text{O}_2$
Galactose oxidase	Galactose oxidation (oxidation of primary alcohols to aldehydes in sugars) (reduction of O <sub>2</sub> to H <sub>2</sub> O <sub>2</sub> )	$\text{RCH}_2\text{OH} + \text{O}_2 \longrightarrow \text{RCHO} + \text{H}_2\text{O}_2$
Cu, Zn-superoxide dismutase	Free radical scavenging	$2\text{O}_2^- + 2\text{H}^+ \longrightarrow \text{H}_2\text{O}_2 + \text{O}_2$
Nitrous oxide reductase	Reduction of N <sub>2</sub> O to N <sub>2</sub>	$\text{N}_2\text{O} \longrightarrow \text{N}_2$

### 1.5.1. Types of copper enzymes

Copper containing enzymes were classified according to their structural, spectroscopic behaviour and distinctive properties into three major types (Table 1.4).<sup>2</sup> Type(I) contains mononuclear copper site and two characteristic

properties: strong electron absorption and distinctive EPR signal with narrow hyperfine coupling and high redox potentials. Type(II) contains weak absorption and shows a four line EPR signal with larger hyperfine splitting patterns and more negative reduction potentials compared to type(I).<sup>7</sup> Type(III) contains dinuclear site and consists of two antiferromagnetically coupled Cu atoms (EPR for two coupling copper ions).<sup>21,68</sup>

**Table 1.4** Type I, II, and III of biological copper sites in most copper proteins, geometry, and chemical structure for specific examples.<sup>4,7,8,61,66</sup>

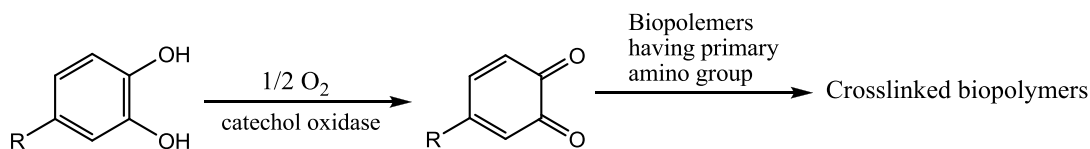
Center	# Cu	Geometry	Example	Structure
Type I	1	Tetrahedral, Trigonal bipyramidal	Plastocyanin	 <p>R= Met, Gln, Glu</p>
Type II	1	Square pyramidal	Cu, Zn SOD	 <p>L= His, Glu, Met, Tyr</p>
Type III	2	Trigonal bipyramidal	Hemocyanin	 <p>L= His X= other ligands or O<sub>2</sub><sup>2-</sup> R= H, alkyl or aromatic</p>

## 1.6. Catalytic activities of copper complexes

Copper complexes have wide range of oxidation and oxygenation catalytic activities of organic substrates (carbohydrates, amines, phenols),<sup>76</sup> as well as several catalytic applications in industry. The copper containing enzymes have several catalytic and biological activities as mentioned in **Table 1.3**. Many mononuclear and binuclear copper complexes have been synthesized as models to mimic the catalytic and biological activities of these enzymes such as: catechol oxidase, phenoxazinone synthase, SOD and other catalytic activities.<sup>77,78</sup>

### 1.6.1. Catechol oxidase (CO)

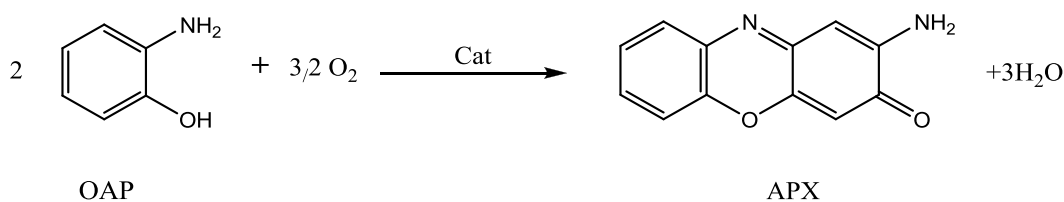
Catechol oxidase is classified as type(III) copper protein that include two copper centres. Each copper(II) ion is coordinated by three histidine residues and bridged by a hydroxide ion in the native met state (**Figure 1.5**).<sup>62</sup> Catechol oxidase has achieved a selective oxidation of catechols to the corresponding o-quinones by catecholase activity process. This process thought to protect a damaged tissue against pathogens and insects.<sup>79</sup> These quinones are highly reactive and undergo auto polymerization to yield polyphenolic pigments as products (**Scheme 1.1**). Melanin that is found in the humans skin and hair is one of these produced pigments which is used to protect the tissue against radiation and desiccation.<sup>80</sup>



**Scheme 1.1** Conversion of catechol to corresponding *o*-quinone, which subsequently undergoes auto polymerization.<sup>81</sup>

### 1.6.2. Phenoxazinone synthase

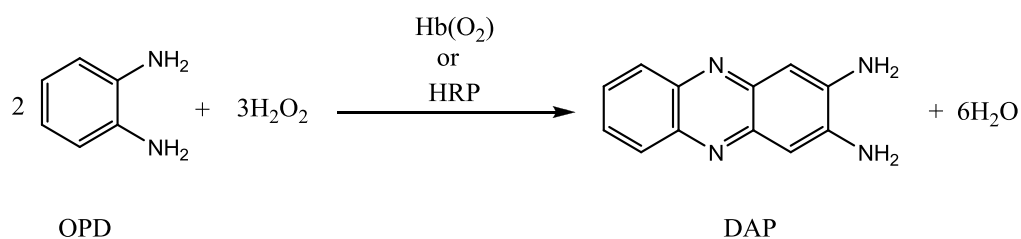
Oxidation of *o*-aminophenol (OAP) to 2-amino-3*H*-phenoxazine-3-one (APX) is quite interesting toward activation of oxygen and oxidation reaction of aromatic amines in human (**Scheme 1.2**).<sup>82</sup> Many copper(II) complexes have been synthesized as models for phenoxazinone synthase (PHS), a type(II) copper protein. It catalyzes the oxidative coupling of two molecules of substituted *o*-aminophenol to the phenoxazinone chromophore in the final step at the biosynthesis of actinomycin D.<sup>83</sup> The latter is clinically used for the treatment of Wilm's tumor, gestational choriocarcinoma and certain types of cancer.<sup>77,84</sup>



**Scheme 1.2** Overall equation of the oxidation of *o*-aminophenol (OAP) to 2-amino-3*H*-phenoxazin-3-one using copper complexes as a catalyst.<sup>83,76</sup>

### 1.6.3. Oxidation of *o*-phenylenediamine

Oxidation of *o*-phenylenediamine (OPD) to 2,3-diaminophenazine (DAP) (**Scheme 1.3**) by transition metal ion and/or complexes such as iron(III), Co(III), Mn(III) and Cu(II),<sup>85</sup> has been reported. DAP is quite interesting due to its useful application in analytical chemistry such as in catalytic analyte, in immunoassay determination of enzyme-catalyzed reactions and others.<sup>86</sup> Copper complexes have been synthesized to mimic the catalytic function of peroxidases<sup>87,88</sup> which are heme-containing protein like hemoglobin (Hb(O<sub>2</sub>)), Horseradish peroxidase, and cytochrome that catalyze the oxidation of various organic and inorganic compounds such as aromatic phenols and amines by hydrogen peroxide.



**Scheme 1.3** Oxidation of OPD to DAP using Horseradish peroxidase or hemoglobin as a catalyst.<sup>89,90</sup>

### 1.7. The aim of the present work

This work is a continuation of the work of Dr. Abuhijleh on the synthesis of Cu-NSAIDs complexes with nitrogen donor ligands as a models for copper containing enzymes. The main results achieved in this thesis are: **(I)** Three new copper(II) complexes of anti-inflammatory drug with nitrogen-based ligands are synthesized:  $[\text{Cu}(\text{sal})_2(\text{pyrazole})_2]$  **(1)**,  $[\text{Cu}(\text{nap})_2(\text{pyrazole})_4]$  **(2)**,  $[\text{Cu}_2(\text{nap})_2(\text{metnd})_2]$  **(3)** **(II)** Spectral and magnetic studies are used to characterization these complexes such as magnetic susceptibility measurements, Uv-Visible and IR-spectroscopies, and X-ray crystallography. **(III)** The biological activities of these new complexes for the oxidation of organic phenols and phenol amines are used to mimic the activities of copper-containing enzymes catecholase and phenoxazinone synthase. **(V)** The effect of solvent on catecholase activity of these complexes is also obtained in different solvents: methanol, dichloromethane and acetonitrile.



## 2. EXPERIMENTAL SECTION

### 2.1. Reagents and materials

Tetrakis- $\mu$ -aspirinato dicopper(II)  $[\text{Cu}_2(\text{asp})_4]$  and tetrakis( $\mu$ -naproxenato) dicopper(II)  $[\text{Cu}_2(\text{nap})_4]$  were prepared according to a published procedure.<sup>91,26</sup> Sodium naproxenate was obtained from Birzeit Pharmaceutical Company (West Bank-Palestine). Acetone, dichloromethane and methanol were obtained from commercial sources. All other chemicals and solvents used in this study were of high purity grade (Aldrich or Sigma chemicals) and were used without further purification.

### 2.2. Physical measurements

Melting points of the complexes were determined in capillary tubes using Electrothermal Melting Point Apparatus without any corrections. Magnetic moments of the complexes were determined by Gouy method by packing the powdered sample into small tube. Mercury cobalt-thiocyanate ( $\text{HgCo}(\text{NCS})_4$ ) was used as a magnetic susceptibility calibrant, and corrected for diamagnetism with the appropriate Pascal constant. The effective magnetic moment was calculated from the expression:  $\mu_{\text{eff}} = 2.84 [(\chi_m)(T)]^{1/2}$  (where  $\chi_m$  is the molar susceptibility and T is the temperature in K). Infrared (IR) spectra in the range  $4000\text{-}200\text{ cm}^{-1}$  were recorded on a Varian 600 FT-IR spectrometer with samples prepared as KBr disk. Electronic spectra and the

catalytic activities were obtained spectrophotometrically with Hewlett Packard 8433A diode array spectrophotometer in the 190-1100 nm region using different solvent.

### 2.3. Synthesis of copper(II) complexes

#### 2.3.1. Synthesis of [Cu(sal)<sub>2</sub>(pz)<sub>2</sub>] (1)

A (0.546 g, 8.00 mmol) of pyrazole dissolved in 10 ml dichloromethane was added gradually to stirring (1.69 g, 2.00 mmol) sample of [Cu<sub>2</sub>(asp)<sub>4</sub>] in 15 ml of the same solvent, then 12 ml of MeOH was added to solution. The resulted blue solution was filtered and left in the hood to evaporate. In dichloromethane, a blue powder is soluble while green powder is slightly soluble, so a mixture of blue and green powders can be separated in this solvent. The blue powder was recrystallized from a mixture of acetone/chloroform (1:1). Yield: 86.5%. m.p. (178-183) °C; UV-Vis:  $\lambda$ /nm ( $\epsilon$ /L mol<sup>-1</sup> cm<sup>-1</sup>); in MeOH: 656 (65.8), 301 (7382), 232 (16018), 205 (62142); IR (KBr, cm<sup>-1</sup>): 3280, 3160, 1605, 1585, 1495, 1460, 1380, 1350, 1290, 1230, 1100, 1020, 840, 762, 680, 580, 470, 360, 275, 200;  $\mu_{\text{eff}} = 1.87$  BM. The complex is soluble in acetone, MeOH, DMSO, acetonitrile and dioxane.

### 2.3.2. Synthesis of [Cu(nap)<sub>2</sub>(pz)<sub>4</sub>] (2)

A (0.273 g, 4.00 mmol) of pyrazole dissolved in 10 ml MeOH was added gradually to stirring (1.04 g, 1.00 mmol) sample of [Cu<sub>2</sub>(nap)<sub>4</sub>] in 15 ml dichloromethane for 1 h. The blue solution was filtered and left in the hood to evaporate to give sky blue precipitate. Suitable crystals obtained for crystal structure determination were obtained from recrystallization of the sky blue precipitate from a mixture of dichloromethane/chloroform (1:1). Yield: 98%. m.p. (133-137) °C; Uv-Vis:  $\lambda$ /nm ( $\epsilon$ / L mol<sup>-1</sup>cm<sup>-1</sup>); in MeOH: 605( 80 ), 331 (4960), 317 (4497), 304 (3167 ), 281 (8419 ), 271 (13203 ), 262 (14187), 231 (145082); IR (KBr, cm<sup>-1</sup>): 3160, 3085, 3090, 2960, 2860, 1690, 1592, 1510, 1545, 1485, 1460, 1440, 1390, 1372, 1345, 1255, 1145, 1105, 1045, 870, 750, 460;  $\mu_{\text{eff}} = 1.77$  BM. The complex is soluble in methanol, ethanol, acetone, dichloromethane and acetonitrile.

### 2.3.3. Synthesis of [Cu<sub>2</sub>(nap)<sub>4</sub>(mtnD)<sub>2</sub>] (3)

A (0.684 g, 4.00 mmol) of metronidazol dissolved in 12 ml of MeOH was added drop wise to stirring (1.04 g, 1.00 mmol) sample of [Cu<sub>2</sub>(nap)<sub>4</sub>] in 15 ml of dichloromethane for 3 h. The green solution was filtered and left in the hood to evaporate to give green precipitate. Yield: 94%. Uv-Vis:  $\lambda$ /nm ( $\epsilon$ / L mol<sup>-1</sup> cm<sup>-1</sup>); in MeOH: 695 (397), 331 (19263), 316 (24571), 281 (23402), 272 (294489), 262 (29660), 252 (27520), 234 (161122), 224 (161229); IR (KBr, cm<sup>-1</sup>): 3385, 3040,

2920, 2830, 1605, 1525, 1450, 1425, 1390, 1340, 1320, 775, 1240, 1155, 1000, 900, 815, 445, 215, 215, 200;  $\mu_{\text{eff}} = 1.39$  BM. The complex is soluble in DMSO, dichloromethane, acetonitrile, chloroform and dioxane.

#### 2.4. X-ray crystallography

Single crystals suitable for X-ray measurements of the complexes **1** and **2** were attached to a glass fiber, with epoxy glue, and transferred to a Bruker SMART APEX CCD X-ray diffractometer system controlled by a Pentium-based PC running the SMART software package.<sup>92</sup> The crystal was mounted on the three-circle goniometer with  $\chi$  fixed at  $+54.76^\circ$ . The diffracted graphite-monochromated Mo  $K\alpha$  radiation ( $\lambda = 0.71073$  Å) was detected on a phosphor screen held at a distance of 6.0 cm from the crystal operating at  $-43^\circ\text{C}$ . A detector array of 512 X 512 pixels, with a pixel size of approximately 120  $\mu\text{m}$ , was employed for data collection. The detector centroid and crystal-to-detector distance were calibrated from a least-squares analysis of the unit cell parameters of a carefully centered YLID reference crystal. After the crystal of the complex had been carefully optically centered within the X-ray beam, a series of 30 data frames measured at  $0.3^\circ$  increments of  $\omega$  were collected with three different  $2\theta$  and  $\phi$  values to assess the overall crystal quality and to calculate a preliminary unit cell. For the collection of the intensity data, the detector was positioned at a  $2\theta$  value of  $-28^\circ$  and the intensity images were measured at

0.3° intervals of  $\omega$  for duration of 20 sec. each. The data frames were collected in four distinct shells which, when combined, measured more than 1.3 hemispheres of intensity data with a maximum  $2\theta$  of 46.5°. Immediately after collection, the raw data frames were transferred to a second PC computer for integration by the SAINT program package.<sup>93</sup> The background frame information was updated according to the equation  $B' = (7B+C)/8$ , where  $B'$  is the update pixel value,  $B$  is the background pixel value before updating, and  $C$  is the pixel value in the current frame. The integration was also corrected for spatial distortion induced by the detector. In addition, pixels that reside outside the detector active area or behind the beam stop were masked during frame integration. The integrated intensities for the four shells of data were merged to one reflection file. The data file was filtered to reject outlier reflections. The rejection of a reflection was based on the disagreement between the intensity of the reflection and the average intensity of the symmetry equivalents to which the reflection belongs. In the case of strong reflections ( $I > 99\sigma(I)$ ) which contains only two equivalents, the larger of the two equivalents was retained. The structure was solved and refined by the SHELXTL software package.<sup>94</sup> Crystal data and more details of the data collections and refinements are summarized in **Table 2.1** for **1** and **2**. Selected bond lengths and angles for **1** and **2** are summarized in **Table 2.2** and in **Table 2.3**, respectively.

**Table 2.1** Data and structure refinement for **1** and **2**.

	Complex 1	Complex 2
Empirical formula	C <sub>20</sub> H <sub>18</sub> CuN <sub>4</sub> O <sub>6</sub>	C <sub>40</sub> H <sub>42</sub> CuN <sub>8</sub> O <sub>6</sub>
Formula weight	473.92	794.36
Temperature	293(1) K	293(1) K
Wavelength	0.71073 Å	0.71073 Å
Crystal system	Monoclinic	Monoclinic
Space group	P2(1)/n	P2(1)
a	5.1347(5) Å	8.630(2) Å
b	20.532(2) Å	25.675(5) Å
c	9.6258(8) Å	8.782(2) Å
α	90°	90°
β	104.510(1)°	94.071(3)°
γ	90°	90°
Volume	982.4(2) Å <sup>3</sup>	1941.0(6) Å <sup>3</sup>
Z	2	2
Density (calculated)	1.602 Mg/m <sup>3</sup>	1.359 Mg/m <sup>3</sup>
Absorption coefficient	1.159 mm <sup>-1</sup>	0.620 mm <sup>-1</sup>
F(000)	486	830
Crystal size	0.34 x 0.12 x 0.08 mm <sup>3</sup>	0.28 x 0.26 x 0.21 mm <sup>3</sup>
Theta range for data collection	2.95 to 28.00°	2.33 to 27.00°
Reflections collected	11271	21581
Independent reflections	2341 [R(int) = 0.0253]	8348 [R(int) = 0.0280]
Completeness to theta = 28.00°	98.9 %	99.4 %
Absorption correction	None	None
Refinement method	Full-matrix least-squares on F <sup>2</sup>	Full-matrix least-squares on F <sup>2</sup>
Data / restraints / parameters	2341 / 0 / 142	8348 / 5 / 512
Goodness-of-fit on F <sup>2</sup>	1.236	1.037
Final R indices [I>2σ(I)]	R1 = 0.0518, wR2 = 0.1173	R1 = 0.0445, wR2 = 0.1153
R indices (all data)	R1 = 0.0556, wR2 = 0.1193	R1 = 0.0542, wR2 = 0.1207
Largest diff. peak and hole	0.384 and -0.301 e.Å <sup>-3</sup>	0.346 and -0.263 e.Å <sup>-3</sup>

**Table 2.2** Selected bond lengths (Å) and bond angles (°) for complex **1**

	Bond distance (Å)		Bond angle (°)
Cu(1)-N(1)	1.974(2)	N(1)#1-Cu(1)-O(1)	89.73(9)
Cu(1)-N(1)#1	1.974(2)	N(1)-Cu(1)-O(1)#1	89.73(9)
Cu(1)-O(1)	1.9766(17)	N(1)#1-Cu(1)-O(1)#1	90.27(9)
Cu(1)-O(1)	1.9766(17)	O(1)-Cu(1)-O(1)#1	180.000(1)
Cu(1)-O(1)#1	1.9766(17)	C(10)-N(1)-Cu(1)	131.5(2)
Cu(1)-O(2)	2.602	N(1)-Cu(1)-N(1)#1	180.000(1)
N(2)-H(1N2)	0.8540	N(1)-Cu(1)-O(1)	90.27(9)
C(7)-O(2)	1.233(3)	N(2)-C(8)-C(9)	107.8(3)
C(7)-O(1)	1.298(3)	N(2)-C(8)-H(8)	121.9
N(1)-N(2)	1.346(3)	N(1)-C(10)-C(9)	110.9(3)
N(2)-H(1N2)	0.8540	N(1)-C(10)-H(10)	121.8

**Table 2.3** Selected bond lengths (Å) and bond angles (°) for complex **2**.

	Bond distance (Å)		Bond angle (°)
Cu(1)-N(7)	2.014(2)	N(7)-Cu(1)-N(3)	179.53(11)
Cu(1)-N(3)	2.014(2)	N(7)-Cu(1)-N(1)	90.96(9)
Cu(1)-N(1)	2.019(2)	N(3)-Cu(1)-N(1)	89.34(10)
Cu(1)-N(5)	2.031(2)	N(7)-Cu(1)-N(5)	89.63(10)
Cu(1)-O(1)	2.389(3)	N(3)-Cu(1)-N(5)	90.06(10)
Cu(1)-O(4)	2.490(2)	N(1)-Cu(1)-N(5)	178.64(12)
N(4)-H(4N)	0.890(10)	N(7)-Cu(1)-O(1)	88.54(13)
O(1)-H(6N)	2.32(5)	N(3)-Cu(1)-O(1)	91.77(13)
O(2)-H(2N)	1.81(2)	N(1)-Cu(1)-O(1)	98.06(10)
O(4)-H(4N)	2.04(3)	N(5)-Cu(1)-O(1)	83.18(11)
O(5)-H(8N)	2.14(3)	O(1)-Cu(1)-O(4)	173.30(14)

## 2.5. Biological activity studies

### 2.5.1. Catechol oxidase activity

The aerobic oxidation of 3,5-dtbc to the corresponding 3,5-dtbq were carried out in vitro spectrophotometrically by monitoring the formation the qionone at 400 nm ( $\epsilon = 1700 \text{ L mol}^{-1} \text{ cm}^{-1}$ ) in methanol. The catecholase activity of the complexes was determined as micromoles of 3,5-dtbq produced/min/mg of complex. In a typical experiment, 50  $\mu\text{L}$  of the complex solution of ( $2.57 \times 10^{-3} \text{ M}$  for **1**,  $1.50 \times 10^{-3}$  for **2**, and  $1.20 \times 10^{-3} \text{ M}$  for **3**. Complex **3** is dissolved in methanol by using lab sonicator) was added to 1.8 mL of a methanolic solution of 3,5-DTBC ( $9.2 \times 10^{-3} \text{ M}$ ). After shaken the mixture it was placed quickly into 1 cm quartz cell, the absorbance is recorded immediately and every 2 min over a period of 30 min.

A kinetic study of the 3,5-dtbc oxidation reaction by complexes **1-3** was determined by measuring the initial rate using the first few seconds of the oxidation process of absorbance vs. time. Pseudo first-order condition was applied by using various

complex concentrations in  $2 \times 10^{-4}$ – $2 \times 10^{-5}$  M range of **1**,  $2 \times 10^{-3}$ – $1.25 \times 10^{-4}$  M of **2**, and  $2 \times 10^{-3}$ – $2 \times 10^{-4}$  M of **3** while keeping the concentration of 3,5-dtbc substrate is fixed ( $6.88 \times 10^{-3}$  M). On the other hand, various 3,5-dtbc substrate concentrations in  $2 \times 10^{-2}$ – $4 \times 10^{-4}$  M range while keeping the concentration of complexes is fixed ( $2.57 \times 10^{-3}$  M for **1**,  $1.50 \times 10^{-3}$  for **2**, and  $1.20 \times 10^{-3}$  M for **3**).

### 2.5.2. Solvent-dependent catecholase activity

The effect of solvent toward the oxidation of 3,5-DTBC to 3,5-DTBQ by complexes **1-3** was studied under aerobic conditions in different solvents; methanol, dichloromethane and acetonitrile. The reaction was carried out by adding 50  $\mu$ L of  $2.57 \times 10^{-3}$  M of **1**,  $1.50 \times 10^{-3}$  of **2**, or  $1.20 \times 10^{-3}$  M of **3** to 1.8 ml of  $9 \times 10^{-3}$  M of 3,5-dtbc in the desired solvent. The increase in the absorbance at 400 nm, due to 3,5-dtbq formation was recorded immediately after mixing every 90 s over a period of 30 min.

### 2.5.3. Phenoxazinone synthase activity

The aerobic oxidation of OAP to APX by copper complexes in methanol was studied spectrophotometrically by following the formation of APX at 430 nm ( $\epsilon = 2.4 \times 10^4$  L mol<sup>-1</sup>cm<sup>-1</sup>).<sup>78,95</sup> The phenoxazinone synthase activity of the complexes was determined as micromoles of APX produced/min/mg of complex in a similar way as described in Section 2.5.1 using 0.014 M of OAP substrate. A kinetic study of the



OAP oxidation reaction by complexes **1-3** was determined as described in Section 2.5.1. Different complex concentrations in  $2 \times 10^{-4}$ – $2 \times 10^{-5}$  M range for **1**,  $2 \times 10^{-3}$ – $1.25 \times 10^{-4}$  M for **2**, and  $1 \times 10^{-3}$ – $2.2 \times 10^{-4}$  M for **3** were used, while keeping the concentration of OAP substrate is fixed (0.022 M) in order to determine the reaction order in copper complex. On the other hand, various OAP substrate concentrations in  $1.25 \times 10^{-2}$ – $2.5 \times 10^{-4}$  M range were used while keeping the concentration of complex is fixed ( $2.57 \times 10^{-3}$  M for **1**,  $1.50 \times 10^{-3}$  for **2**, and  $1.20 \times 10^{-3}$  M for **3**) were studied to find the order of the oxidation reaction with respect to OAP concentration.

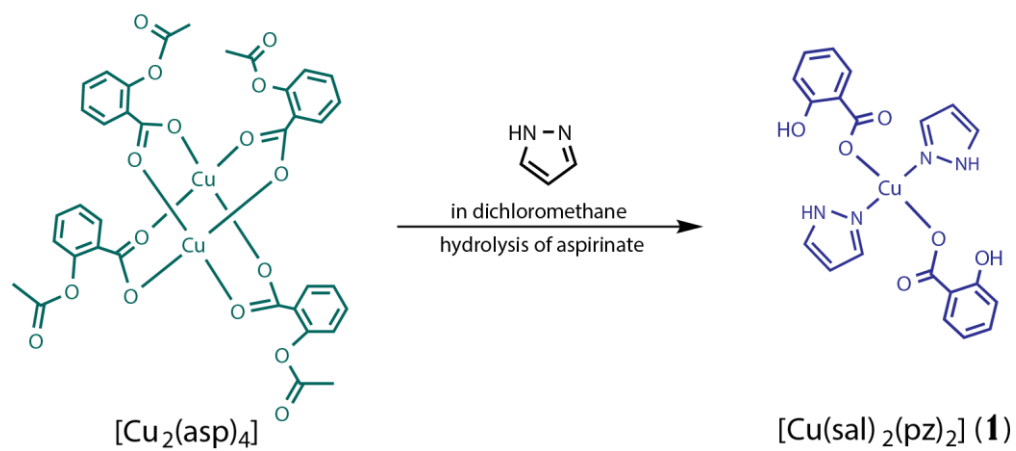
#### **2.5.4. Oxidation of *o*-phenylenediamine activity**

The aerobic oxidation of OPD to APX was studied in methanol spectrophotometrically by following the formation of APX at 430 nm ( $\epsilon = 2.1 \times 10^4$  L mol<sup>-1</sup> cm<sup>-1</sup>).<sup>85</sup> Kinetic studies and the oxidation activity of the complexes, as micromoles of APX produced/min/mg of complex, were determined as described in Section 2.5.3.

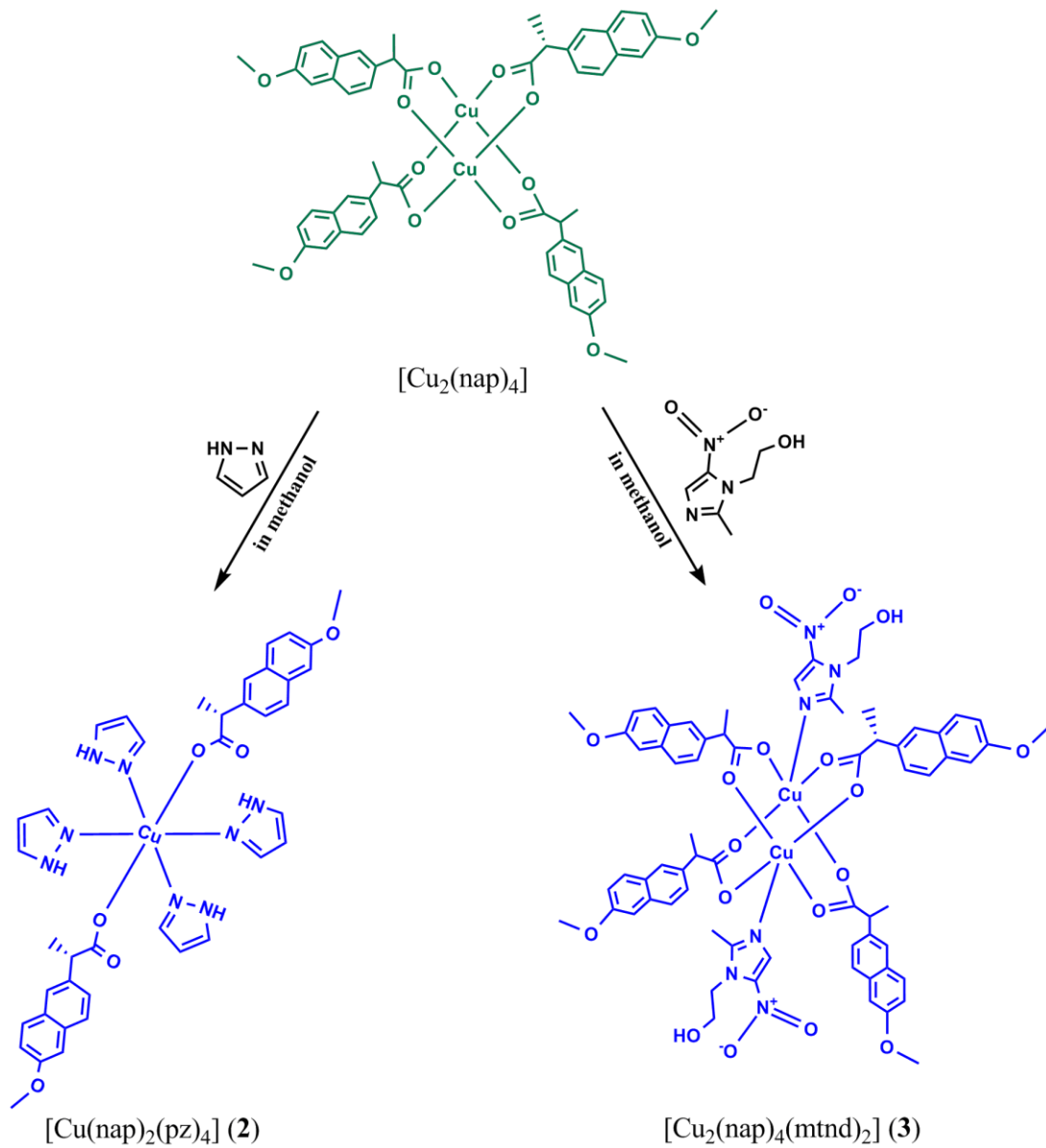
### 3. RESULTS AND DISCUSSIONS

#### 3.1. Synthesis of complexes

Complex **1** has been synthesized as shown in **Scheme 3.1**. The formation of blue solution was produced after mixing both  $[\text{Cu}_2(\text{asp})_4]$  and pyrazole solutions. The solution was left to evaporate to yield green and blue powders (86.5%) as final products. Both powders can be separated by dichloromethane. However, their Uv-Vis bands spectra measurements are similar. This result was attributed to the similarity of these two forms, which can be transformed into each other by using the same solvent such as methanol to give the green solution or acetone to give the blue solution, thus both forms were suggested to be conformational isomers. Complexes **2** and **3** were synthesized by mixing  $[\text{Cu}_2(\text{nap})_4]$  solution with either pyrazole solution to form complex **2** or metronidazole solution to form complex **3** as shown in **Scheme 3.2**. The synthesized complexes **1-3** have been characterized by several physical methods which include magnetic susceptibility measurements, Uv-Vis, IR spectroscopy, and X-ray crystallography.



**Scheme 3.1** The general synthesis of complex **1** at room temperature.



**Scheme 3.2** The general synthesis of complex **2** and **3** at room temperature.

### 3.2. Magnetic and spectroscopic results

The results of magnetic moment measurements for complexes **1-3** are summarized in **Table 3.1**. Complexes **1** and **2** have magnetic moments of 1.85 and 1.77 Bohr Magnetons, respectively at room temperature. These results indicate that each complex contains a paramagnetic Cu(II) centre with one unpaired electron<sup>26,96</sup>. These magnetic moment values are within the range expected for mononuclear copper(II) complexes. Complex **3** has magnetic moment of 1.39 Bohr Magnetons at room temperature. This less than spin only value of magnetic moment (1.73 BM) indicates that spin interactions between copper(II) ion centres occur in this dimeric complex. These interactions will result in an antiferromagnetic behaviour of dimeric copper(II) carboxylate complexes.<sup>7</sup> In a similar results, many of copper carboxylates complexes like  $[\text{Cu}_2(\text{RCOO})_4]$  and  $[\text{Cu}_2(\text{RCOO})_4.L_2]$  were reported previously to have antiferromagnetic behaviour.<sup>7,26,31</sup>

The UV-Vis spectra of complex **1** in methanol solution exhibit one broad band near 656 nm ( $\epsilon = 66 \text{ L mol}^{-1} \text{ cm}^{-1}$ ). This absorbance is assigned to Cu(II) d-d transition and indicates that complex **1** has a structure similar to those mononuclear copper(II) complexes that contain two N-donor ligands, and two O-donor ligands having *trans* or *cis* configuration in the plane of copper(II) and two weakly coordinated O-anions from carboxylate ligands in the axial sites to yield complexes with  $\text{CuN}_2\text{O}_2 + \text{O}_2$  chromophore.<sup>37,50</sup> The d-d electronic transition of complex **2** occurs at 605 nm ( $\epsilon = 80 \text{ L mol}^{-1} \text{ cm}^{-1}$ ). This higher electronic transition energy when compared to that of

complex **1** indicates that complex **2** has a structure similar to those mononuclear copper(II) complexes that contain four N-donor ligands in the plane and two O-donors ligands in the axial sites with  $\text{CuN}_4 + \text{O}_2$  chromophore.<sup>50,37</sup> As expected from the structures of complex **1** and **2**, the latter complex exhibits lower absorbance (higher energy) due to the stronger effect of N-donor than that of the O-donor. The electronic transition of complex **3** in methanol exhibits a broad band near 695 nm ( $\epsilon = 397 \text{ L mol}^{-1} \text{ cm}^{-1}$ ) that is assigned to d-d transition. The electronic transition and the molar absorptivity of complex **3** are evidences that, the complex **3** has a structure similar to those binuclear copper(II) adduct with bridging carboxylate and coordinated axially by N-donors heterocyclic ligands.<sup>96</sup> Unfortunately, the second band (shoulder) in the range 370-420 nm that could be an evidence for the formation of binuclear copper(II) complex is not observed. The broad band observed in the range 300-330 nm ( $\epsilon = 19,000\text{-}26,000 \text{ L mol}^{-1} \text{ cm}^{-1}$ ) can be attributed to LMCT (ligand to metal charge transfer) and to the intra ligand electronic transitions of metronidazole. This indicates that the coordination between copper ion and metronidazole ligands has been achieved.<sup>31,96,97,98</sup>

**Table 3.1** Magnetic and spectral data for the complexes **1-3**

Complex	Magnetic Moment (BM)	$\lambda_{\max}$ (nm)	$\nu_{\text{asy}}(\text{COO}^-)$ ( $\text{cm}^{-1}$ )	$\nu_{\text{sy}}(\text{COO}^-)$ ( $\text{cm}^{-1}$ )	$\Delta \nu$ ( $\text{cm}^{-1}$ )
<b>1</b>	1.85	656	1585	1380	205
<b>2</b>	1.77	605	1592	1378	214
<b>3</b>	1.39	695	1605	1425	179

The IR spectra of complex **1** show absorptions at  $1585 \text{ cm}^{-1}$  assigned to  $\nu_{\text{asy}}(\text{COO})$  and at  $1380 \text{ cm}^{-1}$  assigned to  $\nu_{\text{sy}}(\text{COO})$ . The separation between  $\nu_{\text{asy}}(\text{COO})$  and  $\nu_{\text{sy}}(\text{COO})$ ,  $\Delta\nu$  is  $205 \text{ cm}^{-1}$  (**Table 3.1**). The separation value ( $\Delta\nu$ ) may give some evidence for the coordination mode of carboxylate anion to metal. The  $\Delta\nu$  value in complex **1** is in the range expected for mononuclear copper(II) complexes, that have been reported previously,<sup>42,50</sup> in which the carboxylate groups coordinate to metal in, essentially mono-dentate coordination mode (Section 1.3.1). The absence of carbonyl stretching absorption in the range  $1720\text{-}1770 \text{ cm}^{-1}$  seems to be spectral evidence for the hydrolysis of aspirinato ligand to salicylato in complex **1** (**Scheme 3.1**).<sup>37,92</sup> The bands that are occurred at  $1605$  and  $1230 \text{ cm}^{-1}$  are assigned to  $\nu(\text{C-C})$  vibrations of the aromatic ring and to  $\nu(\text{C-O})$  of the O-H group, respectively, of the salicylate ligand. The  $\nu(\text{C=N})$  of the coordinated pyrazole ligand occurs at  $1460 \text{ cm}^{-1}$ . The broad band that is occurred at  $3240 \text{ cm}^{-1}$  is assigned to  $\nu(\text{N-H})$  of the coordinated pyrazole ligands. The two stretching vibration bands at  $275$  and  $472 \text{ cm}^{-1}$  are assigned to  $\nu(\text{Cu-N})$  of pyrazole ligands and to  $\nu(\text{Cu-O})$  of the carboxylate of salicylato ligands, respectively.<sup>60</sup> The IR spectra of complex **2** show absorptions

bands at  $1592\text{ cm}^{-1}$  assigned to  $\nu_{\text{asy}}(\text{COO})$  and at  $1378\text{ cm}^{-1}$  assigned to  $\nu_{\text{sy}}(\text{COO})$ . The separation between them,  $\Delta\nu$  of  $214\text{ cm}^{-1}$  is higher than that for sodium naproxenate ( $159\text{ cm}^{-1}$ ) and is consistent with those values reported for the coordination of the carboxylate groups in monodentate mode such as copper-naproxenate with 3-pyridylmethanol ligand.<sup>26, 50</sup> The observed  $\nu(\text{C}=\text{N})$  and the  $\nu(\text{N}-\text{H})$  of the coordinated pyrazole ligands to copper ion frequencies occur at  $1435\text{ cm}^{-1}$  and  $3160\text{ cm}^{-1}$ , respectively. The band at  $1255\text{ cm}^{-1}$  can be assigned to the  $\nu(\text{C}-\text{O})$  of the methoxy group of naproxenato ligand. The bands at  $200$  and  $444\text{ cm}^{-1}$  are assigned to  $\nu(\text{Cu}-\text{N})$  of pyrazole ligands and  $\nu(\text{Cu}-\text{O})$  of the carboxylate groups of salicylato ligands, respectively. The IR spectra of complex **3** shows absorptions bands at  $1605\text{ cm}^{-1}$  assigned to  $\nu_{\text{asy}}(\text{COO})$  and  $1425\text{ cm}^{-1}$  assigned to  $\nu_{\text{sy}}(\text{COO})$ . The separation between asymmetric and symmetric ( $\Delta\nu(\text{COO}), 179\text{ cm}^{-1}$ )  $>$   $\Delta\nu$  of that for sodium naproxenate ( $\Delta\nu, 159\text{ cm}^{-1}$ ). This value indicates that complex **3** has structure similar to those reported for binuclear copper(II) carboxylates in which the carboxylate group interacts with metal in bidentate bridging coordination mode like  $[\text{Cu}_2(\text{valp})_4(\text{mtnd})_2]$ <sup>31</sup>. A broad band observed at  $3350\text{ cm}^{-1}$  is assigned to  $\nu(\text{O}-\text{H})$  group of the coordinated metronidazole ligands. The band at  $1537\text{ cm}^{-1}$  that assigned to  $\nu(\text{C}=\text{N})$  for the non-coordinated metronidazole ring is shifted to  $1566$  in complex **3**. The bands near  $190$  and  $435\text{ cm}^{-1}$  are assigned to  $\text{Cu}-\text{N}$  of metronidazole and  $\text{Cu}-\text{O}$  to naproxenato carboxylate groups, respectively.



The stretching vibration of nitro group in complex **3** exhibit two bands at 1545 and 1450  $\text{cm}^{-1}$  which are assigned to the antisymmetric  $\nu_{\text{asy}}(\text{NO}_2)$  and to symmetric  $\nu_{\text{sy}}(\text{NO}_2)$ , respectively.

### 3.3. Crystal structure of complexes

#### 3.3.1. Crystal structure of complex **1**

The crystal structure of complex **1** has been determined by X-ray crystallography as shown in **Figure 3.1**. **Table 2.1** shows the crystallographic data and structure refinement for complexes **1** and **2**. In complex **1** the copper atom is coordinated in *trans*-configuration to two N-atoms from two pyrazole ligands with Cu–N distance of 1.974 Å and two O-atoms from two carboxylate groups of salicylato ligands with Cu–O distance of 1.9766 Å. Selected bond angles around the copper ion plane are:  $\text{N}(1)\#1\text{-Cu}(1)\text{-O}(1) = 89.73(9)^\circ$ ,  $\text{N}(1)\#1\text{-Cu}(1)\text{-O}(1)\#1 = 90.27^\circ$ ,  $\text{O}(1)\text{-Cu}(1)\text{-O}(1)\#1 = 180.000(1)^\circ$ ,  $\text{N}(1)\text{-Cu}(1)\text{-N}(1)\#1 = 180.000(1)^\circ$ . The obtained bond lengths and bond angles for the complex **1** (**Table 2.2**), show a slightly distortion from ideal square values in the plane of copper ion. The structure of **1** is best described as distorted tetragonal and displayed elongation at the Cu–O axial sites of the second oxygen of carboxylato groups of salicylato anion at 2.602 Å due to Jahn-Teller effect. Bond distances between Cu(II) ion and ligands in complex **1** are comparable to those of tetragonally elongated mononuclear copper(II) complexes having *trans*-

$\text{CuN}_2\text{O}_2 + \text{O}_2$  chromophore.<sup>50</sup> This structure is consistent with the spectroscopic results obtained for this complex as discussed above.

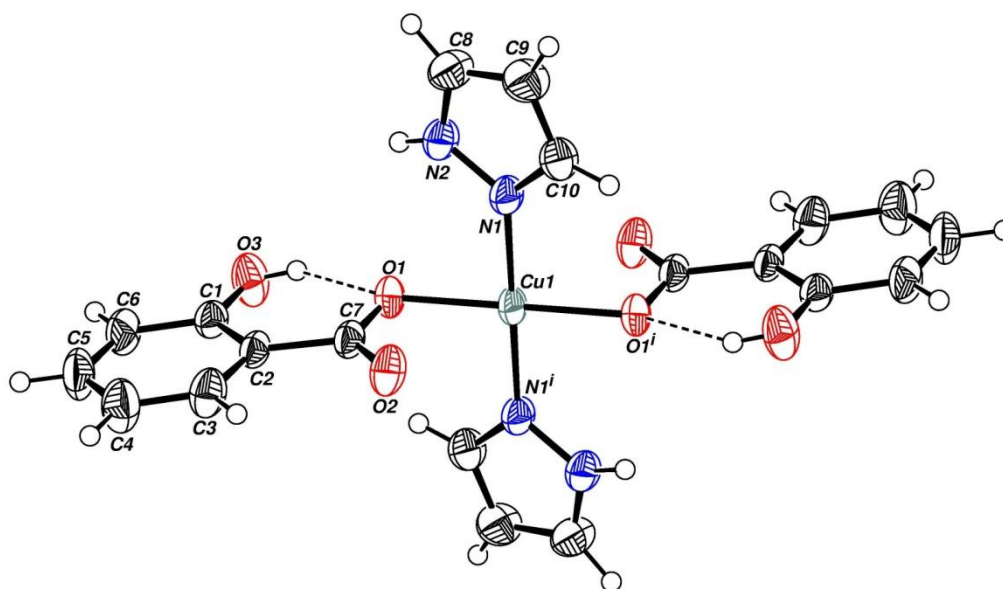


**Figure 3.1** Structure of  $[\text{Cu}(\text{sal})_2(\text{pz})_2]$ , (**1**). Hydrogen atoms have been omitted for clarity.

Complex **1** exhibits two types of hydrogen bonding (**Table 3.2**). The intermolecular hydrogen-bonding between the hydrogen of pyrazole nitrogen ligand and the adjacent carboxylate oxygen of salicylate ligand ( $\text{H}(1\text{N}2)\dots\text{O}(2)\#2 = 2.04 \text{ \AA}$ ,  $\text{N}(2)\text{-H}(1\text{N}2) = 0.85 \text{ \AA}$ ,  $\text{N}(2)\dots\text{O}(2)\#2 = 2.806(3) \text{ \AA}$ ), and the intramolecular hydrogen-bonding between the coordinated oxygen of salicylate ligand and the hydrogen atom of the O-H group in the same salicylate ligand ( $\text{H}(1\text{O}3)\dots\text{O}(1) = 1.90(3) \text{ \AA}$ ,  $\text{O}(3)\text{-}$

H(1O3) = 0.79 Å, O(3)...O(1) = 2.614 Å).

**Table 3.2** Hydrogen bonds for complex **1** [Å and °].

D-H...A	d(D-H)	d(H...A)	d(D...A)	<(DHA)
N(2)-H(1N2)...O(2)#2	0.85	2.04	2.806(3)	149.5
O(3)-H(1O3)...O(1)	0.79	1.90	2.614(3)	149.7

Symmetry transformations used to generate equivalent atoms:

#1 -x+1,-y+1,-z+1 #2 x-1,y,z

### 3.3.2. Crystal structure of complex **2**

The crystal structure of complex **2** is shown in **Figure 3.2**. As expected from magnetic moment, IR and Uv-Vis spectral results, complex **2** has mononuclear structure. However, Cu(II) ion is coordinated to four N-donor atoms from four different pyrazole ligands in the plane, and two O-donor atoms from two naproxenato ligands in the axial sites to yield tetragonally distorted octahedron geometry with  $\text{CuN}_4 + \text{O}_2$  chromophore. The planer Cu-N bond lengths are given in **Table 2.3** (Cu(1)-N(7) = 2.014(2) Å, Cu(1)-N(1) = 2.019(2) Å and Cu(1)-N(5) = 2.031(2) Å ). Selected bond angles between Cu(II) ion and N-donor of pyrazole ligands in the plane are: (N(7)-Cu(1)-N(3) = 179.53(11)°, N(3)-Cu(1)-N(1) = 89.34(10)°, and N(1)-Cu(1)-N(5) = 178.64(12)° and are slightly distorted from ideal angles in square planer. The O-donor anions from the two carboxylate groups of naproxenato ligands in the axial sites have distances of 2.389(3) Å for Cu(1)-O(1)

and 2.490(2) Å for Cu(1)-O(4). Bond distances in complex **2** are comparable to those reported for mononuclear copper(II) complexes having CuN<sub>4</sub>+O<sub>2</sub> and CuN<sub>6</sub> chromophores as in [Cu(Im)<sub>4</sub>(OAc)<sub>2</sub>]<sup>99</sup> and [Cu(Im)<sub>6</sub>](sal)<sub>2</sub>,<sup>100</sup> respectively.

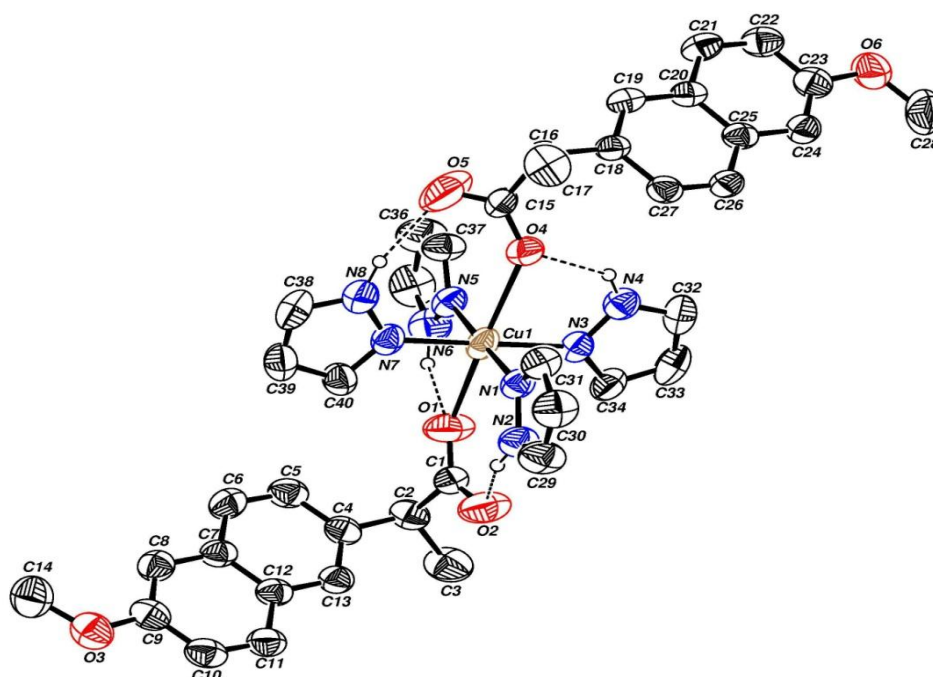


**Figure 3.2** Structure of [Cu(nap)<sub>2</sub>(pz)<sub>4</sub>], (**2**). Hydrogen atoms have been omitted for clarity.

Complex **2** exhibits only intermolecular hydrogen-bonding type (**Table 3.3**) between the uncoordinated nitrogen atom of pyrazole ligands with either coordinated oxygen of naproxenato (H(6N)...O(1) = 2.32(5) Å, N(6)...O(1) = 2.863(5) Å, H(4N)...O(4) =

2.04(3) Å, N(4)...O(4) = 2.771(4) Å, or uncoordinated oxygen of naproxenato (H(8N)...O(5) = 2.14(3) Å, N(8)-H(8N)...O(5) = 2.973(8) Å, H(2N)...O(2) = 1.81(2) Å, N(2)...O(2) = 2.654(5) Å.

**Table 3.3** Hydrogen bonds for complex **2** [Å and °].

D-H...A	d(D-H)	d(H...A)	d(D...A)	<(DHA)
N(8)-H(8N)...O(5)	0.889(10)	2.14(3)	2.973(8)	155(5)
N(6)-H(6N)...O(1)	0.899(10)	2.32(5)	2.863(5)	119(4)
N(4)-H(4N)...O(4)	0.890(10)	2.04(3)	2.771(4)	138(4)
N(2)-H(2N)...O(2)	0.886(10)	1.81(2)	2.654(5)	158(4)

### 3.4. Biological activity studies

#### 3.4.1. Catechol oxidase activity

The synthesized complexes were studied as models for copper-containing enzyme catechol oxidase using Uv-Visible spectroscopy by monitoring the formation of 3,5-dtbq from 3,5-dtbc oxidation at 400 nm in methanol ( $\epsilon = 1700 \text{ L mol}^{-1} \text{ cm}^{-1}$ ). All the complexes show band development at 400 nm as a result of 3,5-dtbc formation (**Figure 3.3**).<sup>31,101</sup>

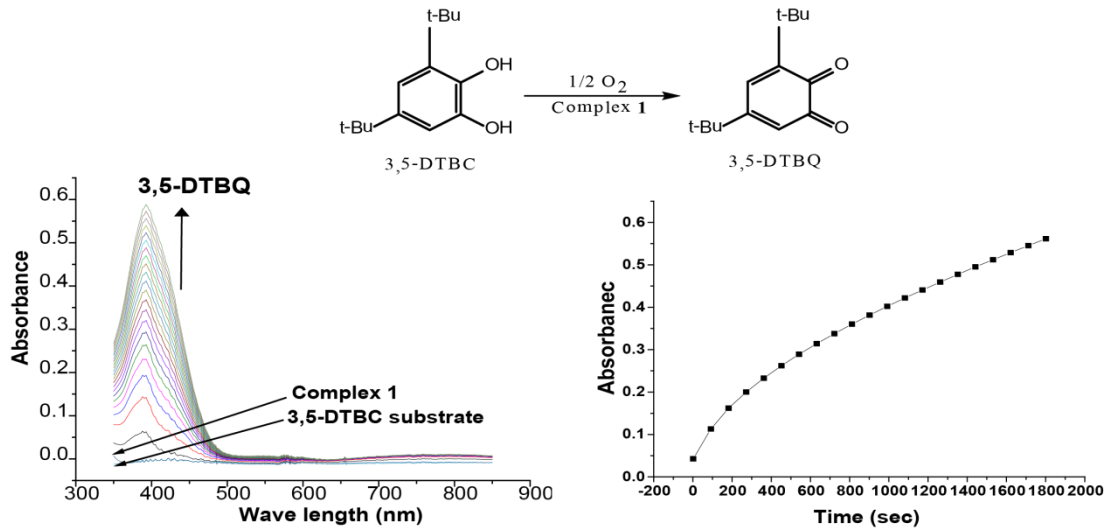


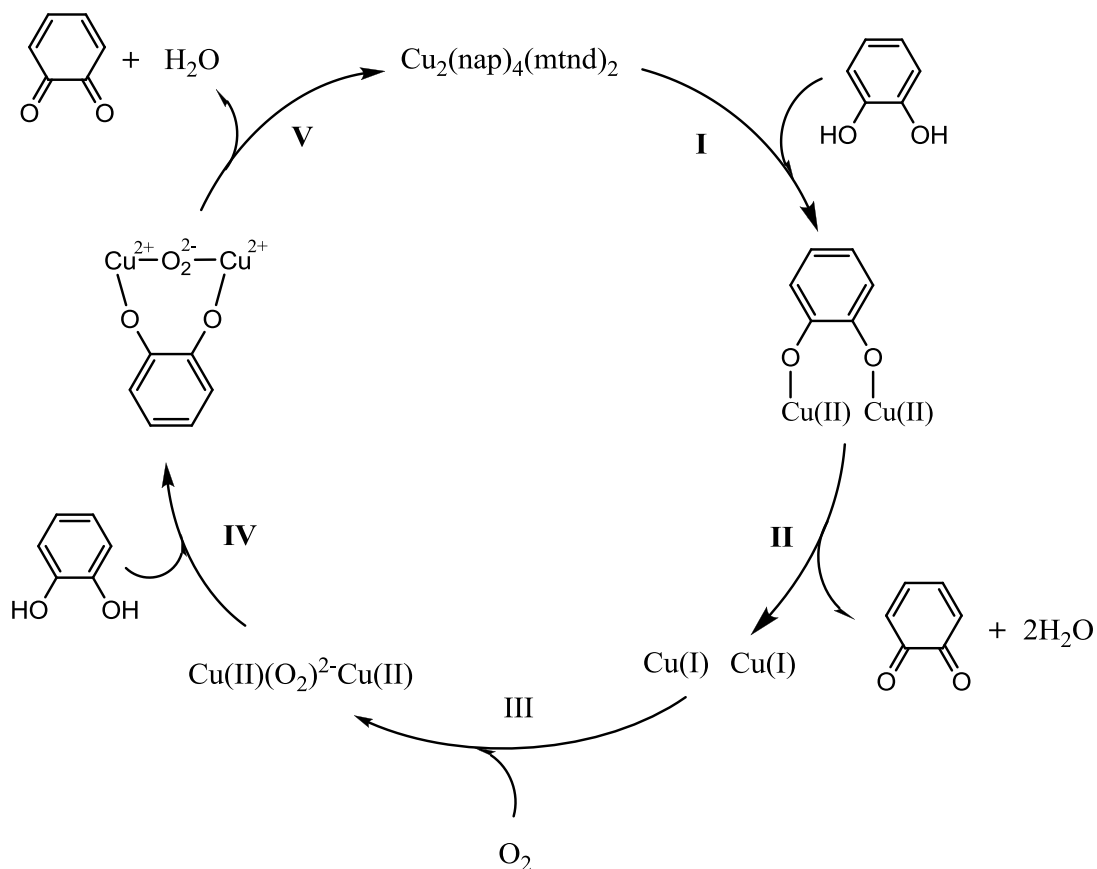
**Figure 3.3** Oxidation of 3,5-dtbc by **1** monitored by Uv-Vis spectroscopy over a period of 30 min and cycle time intervals (90 s) (left). The increase in absorption at 400 nm with time due to 3,5-dtbq formation (right).

The activity of the complexes was determined as micromoles of 3,5-dtbq produced /min/mg of complex.<sup>26,102</sup> The experimental results showed the catecholase activity trends of the three complexes is in the following order: complex **3** > complex **2** > complex **1** in methanol (**Table 3.4**). In general, previous studies showed that binuclear copper complexes have better catecholase activity than mononuclear complexes,<sup>62,67,96</sup> since the naturally occurring enzyme, catecholase is type (III) copper having binuclear structure.<sup>63</sup>

**Table 3.4** Copper complexes activity for the aerobic oxidation of 3,5-dtbc

Complex	Activity ( $\mu\text{mol}/\text{min}/\text{mg cat}$ )
$[\text{Cu}(\text{asp})_2(2\text{-MeIm})_2]^{49}$	0.58
$[\text{Cu}(\text{sal})(2\text{-MeIm})_3]^{49}$	0.69
$[\text{Cu}_2(\text{Nap})_4]^{26}$	1.3
$[\text{Cu}(\text{Nap})_2(3\text{-pym})_2]_n^{26}$	0.35
$[\text{Cu}(\text{Ibup})_2(\text{Im})_2]^{96}$	0.12
$[\text{Cu}_2(\text{Ibup})_4(\text{Mtnd})_2]^{96}$	0.25
Complex 1	0.78
Complex 2	0.92
Complex 3	1.9

The proposed mechanisms for the oxidation of catechols to quinones by mononuclear and dinuclear copper models have been reported previously by Dr. Abuhijleh and other researchers (see Section 1.6.1).<sup>8,26,49,61,62,72,79,103</sup> Briefly, the oxidation process by binuclear Cu(II) complex starts with the chelate coordination of catechol substrate to binuclear copper(II) centres in bidentate bridging mode (**I**) as shown in **Scheme 3.3** to form dicopper catecholato complex. This process is occurred after the dissociation of the carboxylate group from the complex and dehydrogenate the catechol molecule and allow the catecholato group to interact with the catalyst. Internal electron transfer resulted in oxidation of catechol to quinone and reduction of copper centres form (**II**). The reduced copper species interacts with molecular oxygen ( $\text{O}_2$ ) and is then oxidised to a peroxy  $\text{Cu}(\text{II})(\text{O}_2)^{2-}\text{Cu}(\text{II})$  species as a catalytic intermediate (**III**). Another molecule of catechol is coordinated and oxidised to quinone by this peroxy intermediate species and regenerate the initial dicopper(II) complex (**IV**), and (**V**).

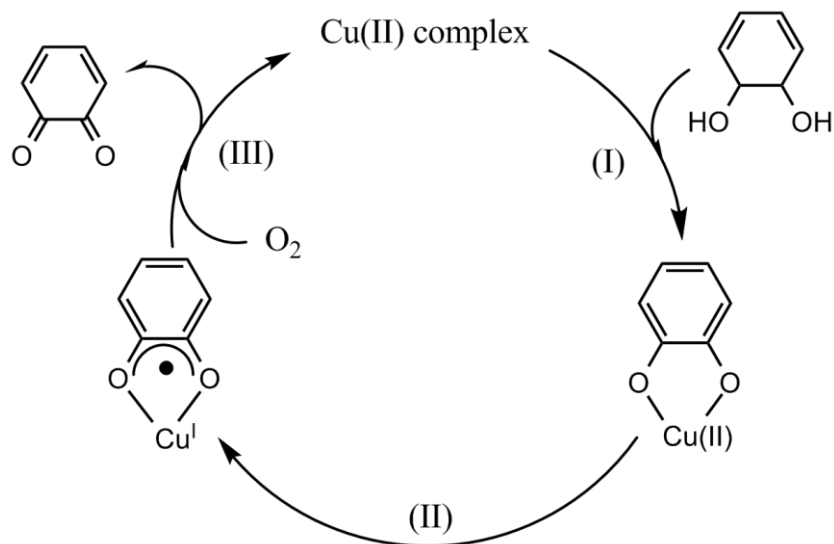


**Scheme 3.3** Proposed mechanism for the oxidation of catechol by dicopper(II) complexes

For the oxidation of catechol by mononuclear copper complexes, the mechanism proceeds via a copper(I) semiquinone radical pathway. This mechanism starts by dissociation of the carboxylato ligands to allow for the catecholato group to coordinate to copper(II) as shown in **(I)** (**Scheme 3.4**). The dissociated carboxylates may be used to dehydrogenate the catechol.<sup>26</sup> An equilibrium occurs through internal electron transfer between  $\text{Cu(II)-(DTBC)}$  and  $[\text{Cu(I)(DTBSQ)}]$  step **(II)**. Oxidation



of the resulted copper(I)-semiquinone species, [Cu(I)(DTBSQ)], by dioxygen releases the quinone product and copper(II) catalyst is regenerated and the catalytic cycle continues **(III)** (**Scheme 3.4**).



**Scheme 3.4** Proposed mechanism for the oxidation of catechol by mononuclear copper(II) complexes

A kinetic study of 3,5-dtbc oxidation reaction by complexes **1-3** was determined by initial rate method using the first few seconds of the oxidation process. Plotting  $\ln$  [initial rates] vs.  $\ln$  [complex], gives straight line with slope value equals 1 which indicates a first-order reaction with respect to complexes (**Figure 3.4** and **Table 3.5**).

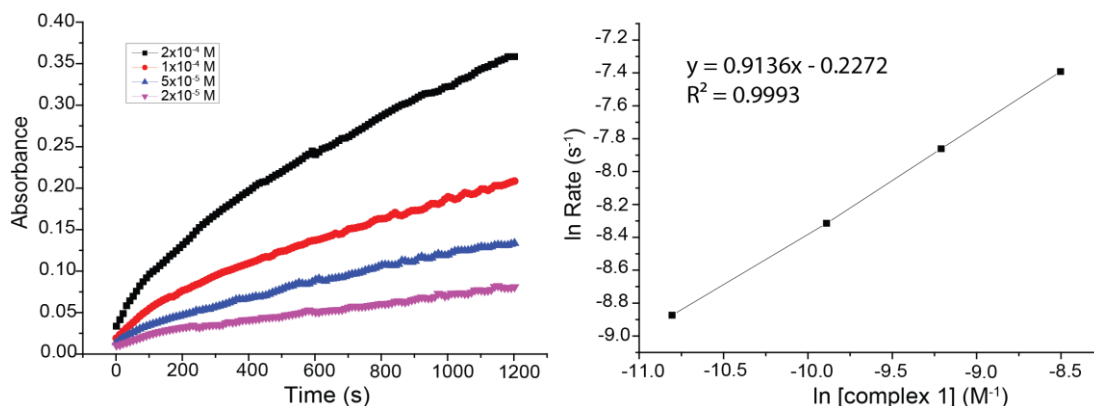


**Figure 3.4** The increase in absorption at 400 nm with time for  $6.9 \times 10^{-3}$  M of 3,5-DTBC that treated with various complex **1** concentrations over a period of 20 min (left). First-order plot for  $\ln \text{Rate (s}^{-1}\text{)}$  verses  $\ln [\text{complex } \mathbf{1}]$  (right)

**Table 3.5** Order of the reaction with respect to complex for the oxidation reaction of 3,5-DTBC, OPD, and OAP substrates by complexes **1-3**

Substrate	Complex <b>1</b>		Complex <b>2</b>		Complex <b>3</b>	
	Order	$R^2$	Order	$R^2$	Order	$R^2$
3,5-DTBC	0.9136	0.9993	1.1951	0.9985	1.1851	0.9997
OAP	0.8976	0.9968	0.9301	0.9997	0.6543	0.9992
OPD	0.7825	0.9996	1.1789	0.9962	1.0587	0.9981

When using various 3,5-dtbc concentration with fixed complex concentration (see Section 2.5.1), a saturation kinetic is observed for complexes **1** and **2** (**Figure 3.5**, right), but for complex **3**, the rate of the reaction seems to be independent of (3,5-dtbc) in (0.001-0.011M) range of concentration.

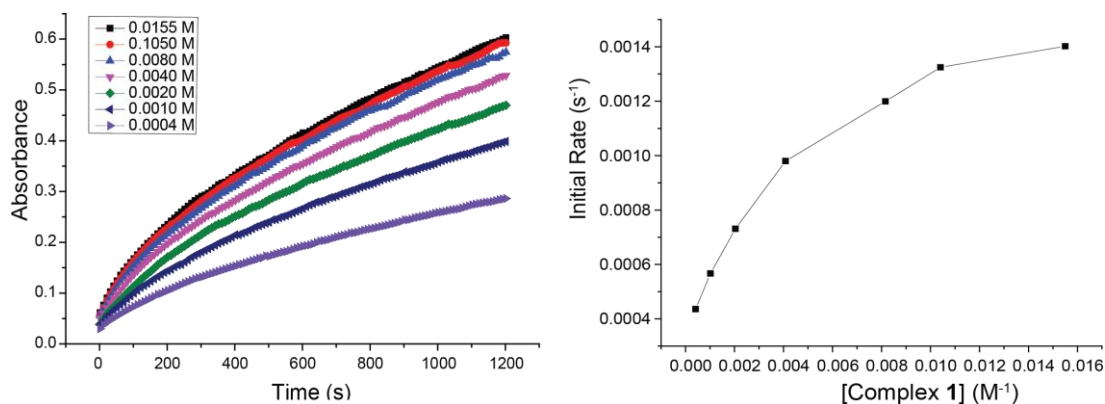


**Figure 3.5** The increase in absorption at 400 nm with time for  $2.57 \times 10^{-3}$  M of complex **1** that treated with various [3,5-dtbc] (left). Plot for initial rate ( $s^{-1}$ ) verses [complex **1**] (right).

### 3.4.2. Solvent-dependent catecholase activity

The catalytic oxidation of of 3,5-DTBC to 3,5-dtbq by copper complexes was studied in different solvents, methanol (MeOH), dichloromethane (DCM), and acetonitrile (ACN). The results of this study showed that the catecholase activities were decreased in the following order: MeOH > DCM > ACN (see **Table 3.6**), (**Figure 3.6**), and (**Figure 3.7**). It has been reported that a protic solvents such as methanol enhance the catechol oxidation more than aprotic solvents such as dichloromethane and acetonitrile.<sup>104,105,106</sup> The O-H hydrogen bondings in protic solvent (methanol) are very strongly solvating the oxygen atoms of carboxylate groups ( $COO^-$ ) which will result in weakening the coordination of the carboxylate anion to Cu(II) ion. This will make the dissociation of the carboxylates group from

the complex is easier and affords available sites at the Cu(II) core for catechol coordination which facilitated the oxidation process.<sup>104,106</sup> On the other hand, the presence of hydrogen bonds in protic solvent may facilitate the hydrogen atom abstraction from catechol which will result in faster formation of copper catecholato intermediate complex, thus increasing the reaction rate of the oxidation process.<sup>106</sup> The oxidation of catechol exhibits lower activity in acetonitrile solvent (**Figure 3.7**). This may indicate that a N-donor ligands, as in acetonitrile, will coordinate to Cu(II) ion and prevent an ease coordination of catechol to copper ion which will hindered and slowed the oxidation process.

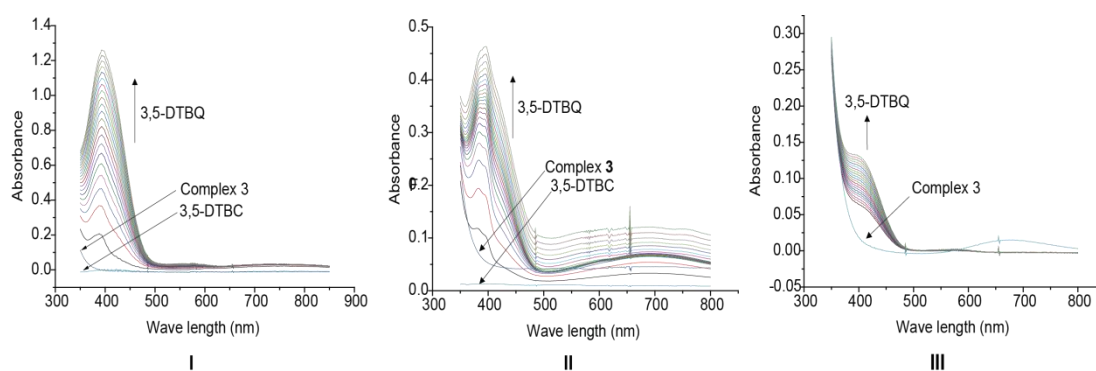


**Figure 3.6** Oxidation of 3,5-dtbc by **3** monitored by Uv-Vis spectroscopy at 400 nm in: **(I)** methanol, **(II)** in dichloromethane, **(III)** in acetonitrile.

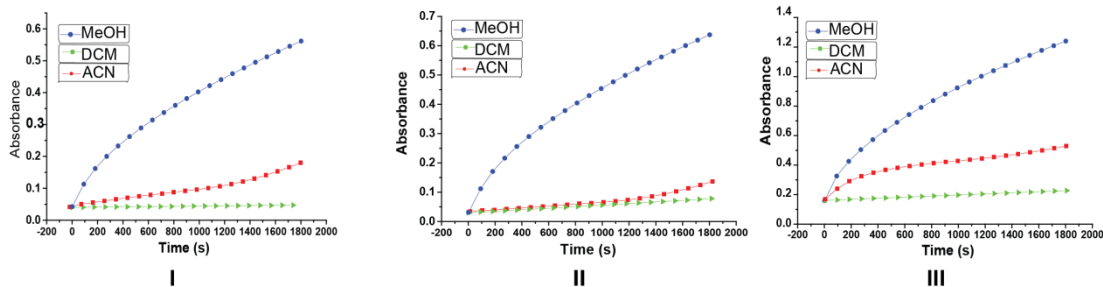


**Figure 3.7** The oxidation of 3,5-DTBC with complex **1 (I)**, complex **2 (II)**, and complex **3 (III)** in different solvents every 2 min over a period of 30 min.

The rate of the oxidation reaction in different solvents was determined by initial rate method as mentioned previously (see **Table 3.6**).

**Table 3.6** Initial rates for the oxidation of 3,5-DTBC in MeOH, CH<sub>2</sub>Cl<sub>2</sub> and acetonitrile by complexes **1-3**

Solvent		<b>1</b>	<b>2</b>	<b>3</b>
MeOH	Initial rate (s <sup>-1</sup> )	$7.8 \times 10^{-4}$	$8.9 \times 10^{-4}$	$1.84 \times 10^{-3}$
DCM	Initial rate (s <sup>-1</sup> )	$9.90 \times 10^{-5}$	$4.08 \times 10^{-5}$	$7.77 \times 10^{-4}$
ACN	Initial rate (s <sup>-1</sup> )	$5.5 \times 10^{-6}$	$2.76 \times 10^{-5}$	$4.19 \times 10^{-5}$

### 3.4.3. Phenoxazinone synthase activity

The synthesized complexes were studied as models for copper-containing enzyme phenoxazinone synthase by studying the oxidation of *o*-aminophenol (OAP) to *o*-amino-3*H*-phenoxazine-3-one (APX). Since APX has characteristic electronic

transition band at about 430 nm, the oxidation process was monitored at this band in methanol solutions ( $\epsilon = 2.4 \times 10^4 \text{ L mol}^{-1} \text{ cm}^{-1}$ ) (**Figure 3.8**).

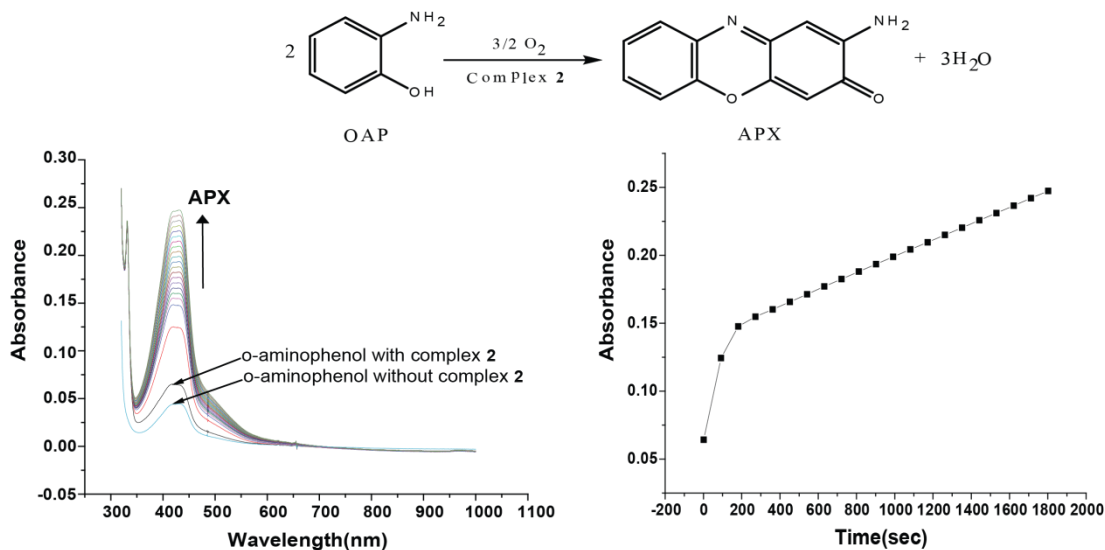


**Figure 3.8** Oxidation of OAP by **2** monitored by Uv-Vis spectroscopy over a period of 30 min and cycle time intervals (90 s) (left). The increase in absorption at 430 nm with time (right)

The activity of the complexes was measured as micromoles of APX produced /min/mg of complex. The catalytic oxidation activity of the complexes was found in the following order: complex **1** > complex **2** > complex **3** as shown in **Table 3.7**. Based on these results, the catalytic activity suggests that the steric hindrance of the coordinated ligands play a major role in the oxidation of OAP to APX. The low catalytic activity of binuclear complex **3** compared to those for mononuclear complexes **1** and **2** may attributed to the presence of four bulky naproxenato-bridged

ligands around the copper centres which hindered the approach of the substrate, *o*-aminophenol to Cu(II) centres resulting in lower oxidation reaction by this complex when compared to other complexes. In complex **1** the carboxylato groups are coordinated-in an essentially monodentate mode to copper atom plane, while the other oxygen atoms of the carboxylate groups weakly coordinated in the axial positions. These carboxylate groups may dissociate and generate vacant sites for *o*-aminophenol coordination and facilitates the oxidation process. In complex **2**, the axial sites are occupied by carboxylate oxygen atoms of the salicylate ligands and may dissociate to allow for *o*-aminophenol coordination to copper(II) to facilitate the oxidation process. The dissociation of the carboxylate groups in complexes **1** and **2** is faster than the dissociation of the bridging carboxylate groups in complex **3** which also attributed to better catalytic activity of the former complexes.

**Table 3.7** Copper complexes activity for the aerobic oxidation of *o*-aminophenol

Complex	Activity ( $\mu\text{mol}/\text{min}/\text{mg cat}$ )
Complex <b>1</b>	0.1660
Complex <b>2</b>	0.0510
Complex <b>3</b>	0.0266

For the kinetic study, the initial rate of the reaction was determined as described in Section 1.6.2, and the order of the reaction with respect to complex as a catalyst is summarized in **Table 3.5**, and was found to be a first order for complexes **1**, and **2**, and may be a half order for complex **3**. Four different concentrations of each

complex have been chosen for studying the effect of complex concentration on the OAP oxidation (**Figure 3.9**).

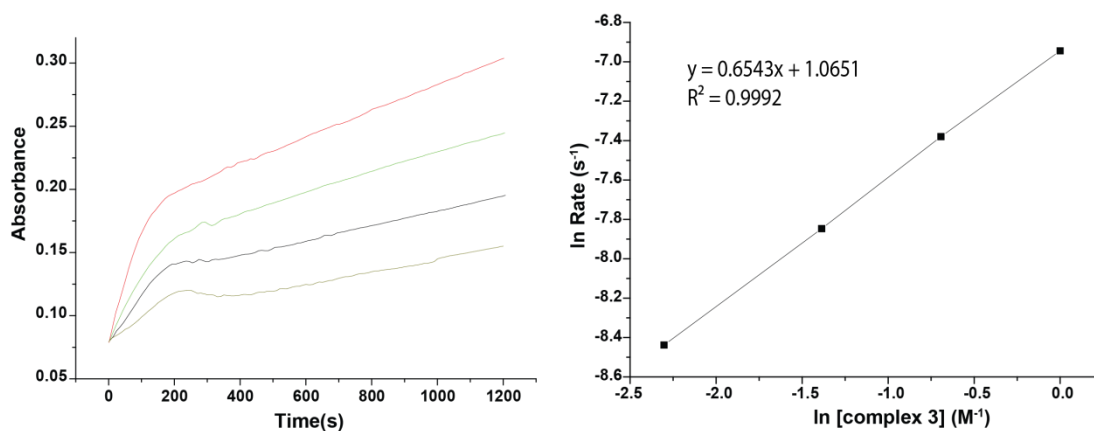


**Figure 3.9** The increase in absorption at 430 nm with time for  $2.2 \times 10^{-2}$  M of OAP that treated with various [complex **3**] every 10 s over a period of 20 min (left). First-order plot for ln Rate (s<sup>-1</sup>) verses ln [complex **3**] (right)

When various OAP concentration in 0.002-0.0002 M range were treated with fixed complex concentration (see Section 2.5.3), the results observed to be independent on OAP concentrations in the ranges (0.001-0.009) for **1**, and **2** and in the range (0.0005-0.0004) for complex **3**.



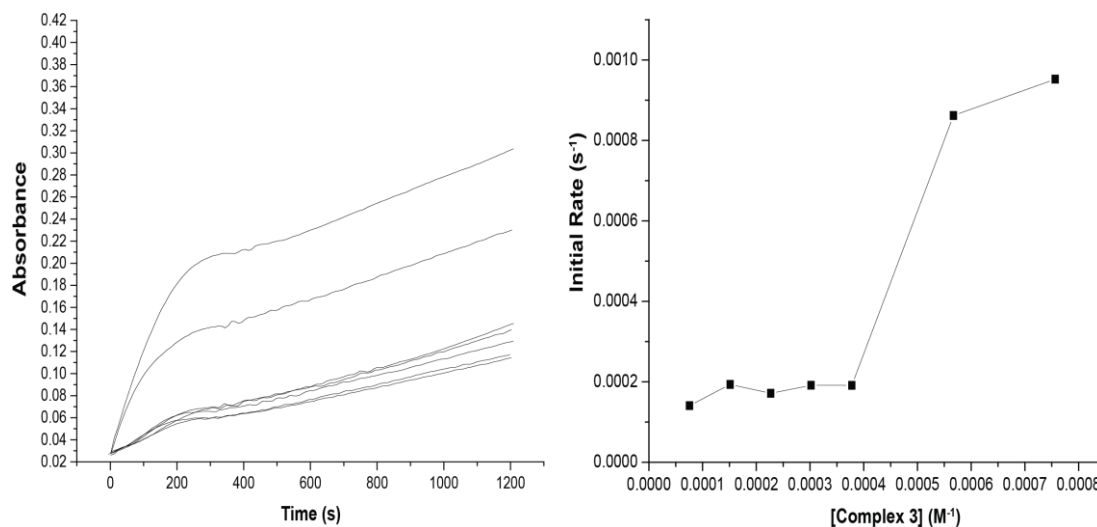
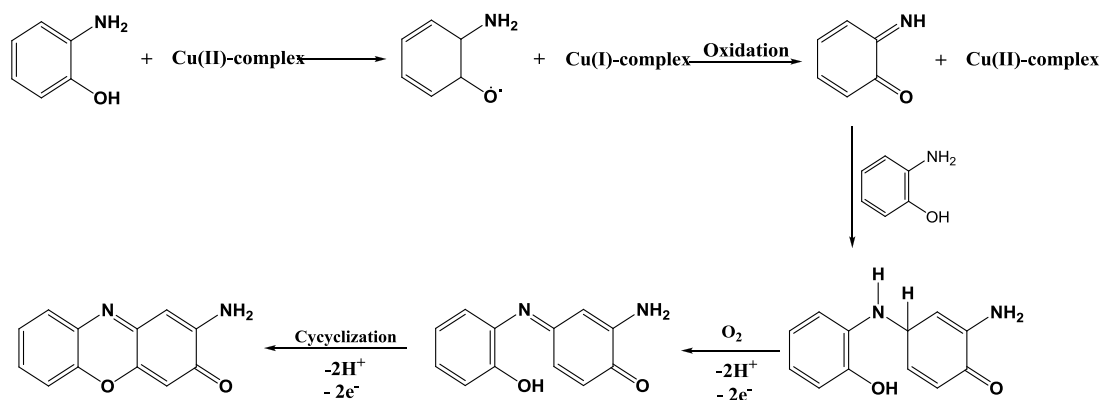


**Figure 3.10** The increase in absorption at 430 nm with time for  $1.20 \times 10^{-3}$  M of complex **3** that treated with various [OAP] (left). Plot for initial rate ( $s^{-1}$ ) verses [complex **3**] (right).

The proposed mechanism for the catalytic oxidation of aromatic amines, *o*-aminophenol (OAP) or *o*-phenylenediamone (OPD-next section), is involving 6-electron oxidation and proceed via radical pathway as in catecholase activity (**Scheme 3.5**). Aromatic amines (OAP or OPD) binds to Cu(II) after its dehydrogenation (by carboxylate groups) to form Cu(II)-OAP(or OPD) complex followed by an internal electron transfer to form Cu(I)-*o*-aminosemiquinone intermediate species. The *o*-aminosemiquinone radical is oxidized to *o*-quinoneimine molecule, which then interacts with another molecule of OAP ( or OPD) to form the product APX (or DAP), after a series of steps, as shown in **Scheme 3.5**.<sup>94,107</sup>



**Scheme 3.5** Proposed reaction mechanism for formation of APX from OAP catalysed by copper(II) complexes.

#### 3.4.4. Oxidation of *o*-phenylenediamine (OPD) to 2,3-diaminophenazine (DAP)

In a similar way, the synthesized complexes were studied as catalyst for the oxidation of OPD to DAP by monitoring the formation of DAP which shows characteristic electronic band at 430 nm in methanol ( $\epsilon = 2.1 \times 10^4 \text{ L mol}^{-1} \text{ cm}^{-1}$ ). All studied complexes (**1**, **2** and **3**) catalyze the oxidation reaction. A represented spectrum for the development of the band at 430 nm due to the catalytic oxidation reaction of OPD to DAP by complex **3** is shown in **Figure 3.11**.

The catalytic activity of the complexes **1-3** as micromoles of DAP produced/min/mg of complex is reported in **Table 3.8**. The results indicate comparable catalytic activity value for the three complexes.

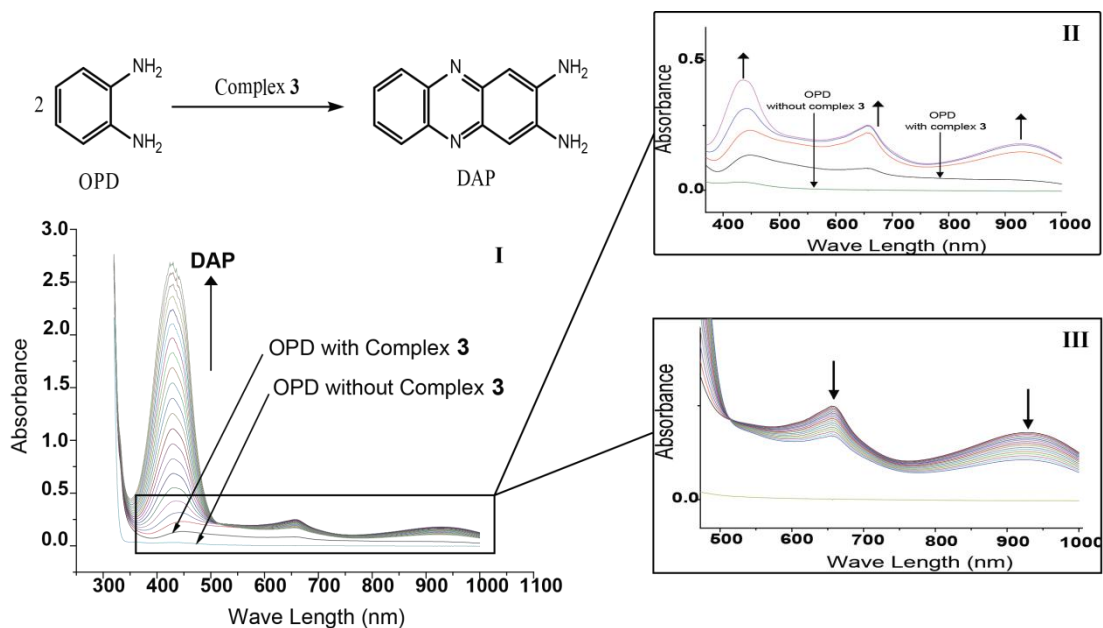


**Figure 3.11** Oxidation reaction of OPD by **3**: (I) the increase in absorbance at 430 nm over a period of 30 min and cycle time intervals 90 s, (II) bands development at 430, 656 and 930 nm after less than one min of mixing OPD and complex **3**, (III) band development at 430 nm continues in increasing after one min of mixing the OPD and complex **3**, while bands at 656 and 930 nm start decaying.

**Table 3.8** Copper complexes activity for the aerobic oxidation of OPD

Complex	Activity ( $\mu\text{mol}/\text{min}/\text{mg cat}$ )
Complex 1	0.063
Complex 2	0.072
Complex 3	0.063

The kinetic study of the OPD oxidation by complexes **1-3** was determined by using initial rate method as described in Section 2.5.4. The catalytic oxidation reaction of

OAP to DAP is approximately first-order in complex **1**, **2** and **3** (Table 3.5). A represented plot for the first order rate is shown in Figure 3.12 for that of complex **1**.

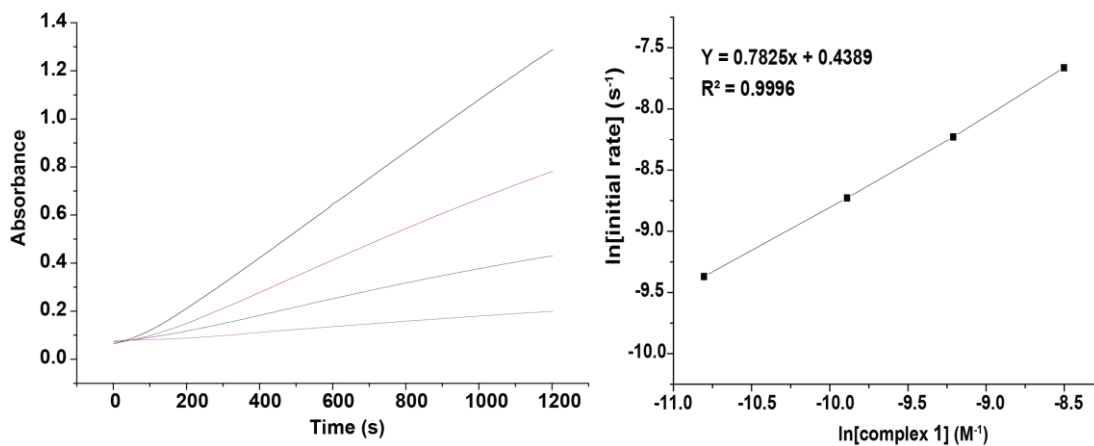


**Figure 3.12** The increase in absorption at 430 nm with time for  $2.2 \times 10^{-2}$  M of OPD that treated with various [complex **1**] in ( $2 \times 10^{-4}$  -  $2 \times 10^{-5}$ ) M range every 10 s over a period of 20 min (left). First-order plot for ln Rate ( $s^{-1}$ ) verses ln [complex **1**] (right)

On the other hand, for a fixed complex concentration, and different OPD concentrations, the reaction order was observed to be almost first order with respect to OPD concentration as shown in Figure 3.13.

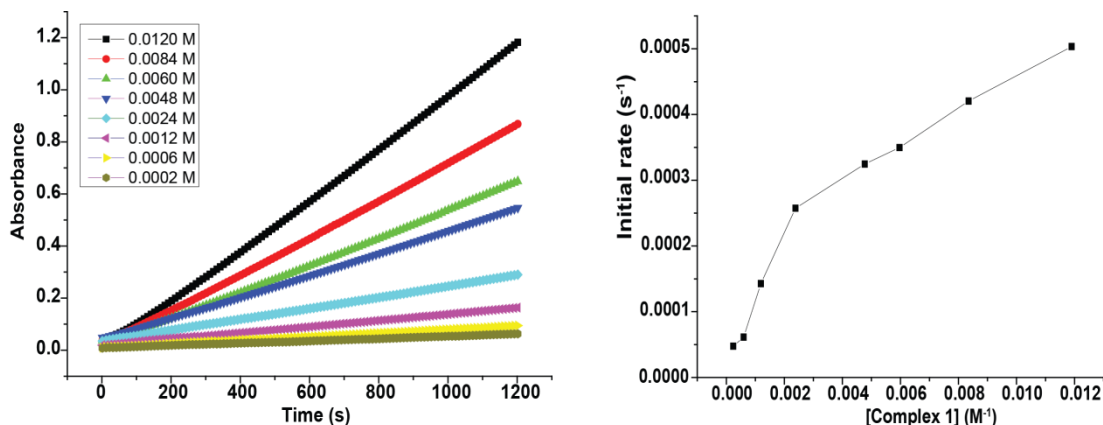
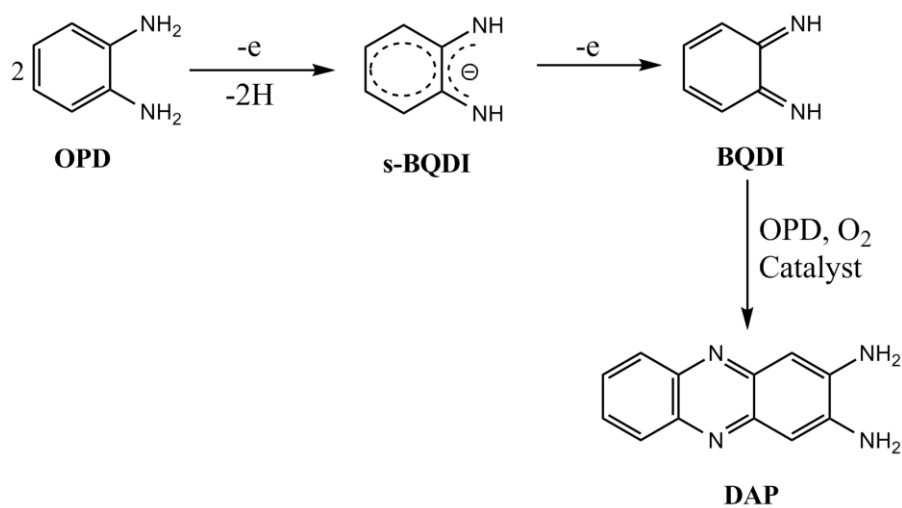


**Figure 3.13** The increase in absorption at 430 nm with time for  $2.57 \times 10^{-3}$  M of complex **1** that treated with various [OPD] (left). Plot for initial rate ( $\text{s}^{-1}$ ) verses [complex **3**] (right).

The proposed mechanism for the formation of DAP from OPD by copper(II) complex models has been reported previously by Dr. Abuhijleh<sup>87</sup> (**Scheme 3.6**). The mechanism proceeds as discussed above for the OAP oxidation via radical pathway intermediate. Oxidation reaction of OPD starts initially by coordination between Cu(II) ion and OPD and an internal electron transfer produced Cu(I) *o*-semibenzoquinonediimine (s-BQDI) species. Oxidation by aerial oxygen produced Cu(II) complex and benzequinonediimine (BQDI) which interacts with another molecule of OPD to form the product DAP, after a series of steps, as shown in **Scheme 3.6**.<sup>84</sup> The two observed bands at 656 and 930 nm in the spectrum of the catalytic oxidation reaction of OPD by complex **3** (**Figure 3.11**) is an indication of the formation of Cu-anionic radical (s-BQDI) intermediate species which has been discussed previously,<sup>87</sup> and as shown in the previous section. The characteristic

bands of anionic radical and its Cu-species intermediate develop initially after mixing both complex and OPD substrate in methanol under aerobic condition. Quickly after one minute of oxidation reaction they start to decay, while the band at 430 nm, due to DAP formation, starts to increase with the formation of an isobestic point at about 510 nm, **Figure 3.11**.<sup>90,85,107</sup>



**Scheme 3.6** Proposed reaction mechanism for the formation of DAP from OPD catalysed by copper(II) complexes

## 4. REFERENCES

- (1) Dudev, T.; Lim, C. *Acc. Chem. Res.* **2006**, *40*, 85.
- (2) MacPherson, I. S.; Murphy, M. E. *Cell Mol Life Sci* **2007**, *64*, 2887.
- (3) Rosenzweig, A. C.; Dooley, D. M. *Curr. Opin. Chem. Biol.* **2006**, *10*, 89.
- (4) Lawrance, G. A. *Introduction to Coordination Chemistry*; Wiley, 2009.
- (5) Gwaltney-Brant, S. M. In *Haschek and Rousseaux's Handbook of Toxicologic Pathology (Third Edition)*; Haschek, W. M., Rousseaux, C. G., Wallig, M. A., Eds.; Academic Press: Boston, 2013.
- (6) Ke, Q.; Costa, M.; Kazantzis, G. In *Handbook on the Toxicology of Metals (Third Edition)*; Nordberg, G. F., Fowler, B. A., Nordberg, M., Friberg, L. T., Eds.; Academic Press: Burlington, 2007.
- (7) Roat-Malone, R. M. *Bioinorganic Chemistry: A Short Course*; Wiley, 2003.
- (8) Peterson, R. L.; Kim, S.; Karlin, K. D. In *Comprehensive Inorganic Chemistry II (Second Edition)*; Reedijk, J., Poeppelemeier, K., Eds.; Elsevier: Amsterdam, 2013.
- (9) Weder, J. E.; Dillon, C. T.; Hambley, T. W.; Kennedy, B. J.; Lay, P. A.; Biffin, J. R.; Regtop, H. L.; Davies, N. M. *Coord. Chem. Rev.* **2002**, *232*, 95.
- (10) Zatta, P.; Frank, A. *Brain Res Rev* **2007**, *54*, 19.
- (11) Hellman, N. E.; Gitlin, J. D. *Annu Rev Nutr* **2002**, *22*, 439.
- (12) Tapiero, H.; Townsend, D. M.; Tew, K. D. *Biomed Pharmacother* **2003**, *57*, 386.
- (13) Bach, J.-P.; Kumar, N.; Depboylu, C.; Noelker, C.; Klockgether, T.; Bacher, M.; Balzer-Geldsetzer, M.; Dodel, R. *J. Neurol. Sci* **2010**, *291*, 95.
- (14) Forte, G.; Alimonti, A.; Violante, N.; Di Gregorio, M.; Senofonte, O.; Petrucci, F.; Sancesario, G.; Bocca, B. *J. Trace Elem. Med Biol.* **2005**, *19*, 195.
- (15) Kaido, T.; Hashimoto, H.; Okamura, H.; Tsukaguchi, K. *J. Clin. Neurosci* **2005**, *12*, 205.
- (16) Uriu-Adams, J. Y.; Keen, C. L. *Mol Aspects Med* **2005**, *26*, 268.
- (17) Brewer, G. J. *Chem. Res. Toxicol.* **2009**, *23*, 319.
- (18) Walshe, J. M. In *Advances in Clinical Chemistry*; Gregory, S. M., Ed.; Elsevier, 2010; Vol. Volume 50.
- (19) Albert, C. F.; Geoffrey, W. *Advanced Inorganic Chemistry: a Comprehensive Text*; Wiley Eastern Limited, 1996.
- (20) Krause, N. *Modern Organocopper Chemistry*; Wiley-VCH, 2002.
- (21) Housecroft, C. E.; Sharpe, A. G. *Inorganic Chemistry*; Pearson Prentice Hall, 2005.
- (22) Greenwood, N. N.; Earnshaw, A. *Chemistry of the elements*; Pergamon Press, 1984.
- (23) Mukherjee, R. In *Comprehensive Coordination Chemistry II*; Editors-in-Chief: , J. A. M., Meyer, T. J., Eds.; Pergamon: Oxford, 2003.
- (24) Anson, F. C.; Collins, T. J.; Richmond, T. G.; Santarsiero, B. D.; Toth, J. E.; Treco, B. G. *R. T. J. Am. Chem. Soc.* **1987**, *109*, 2974.
- (25) Hanss, J.; Krüger, H.-J. *Angewandte Chemie* **1996**, *35*, 2827.
- (26) Abuhijleh, A. L.; Khalaf, J. *Eur. J. Med. Chem* **2010**, *45*, 3811.
- (27) Wang, L.; Guo, B.; Li, H.-X.; Li, Q.; Li, H.-Y.; Lang, J.-P. *Dalton Trans* **2013**.

- (28) Ramakrishnan, C.; Geetha, Y. S. *Proceedings of the Indian Academy of Sciences - Chemical Sciences* **1990**, *102*, 481.
- (29) Nishida, Y.; Takeuchi, M.; Oishi, N.; Kida, S. *Inorg. Chim. Acta* **1985**, *96*, 81.
- (30) Kumar, P.; Kalita, A.; Mondal, B. *Inorg. Chim. Acta* **2013**, *404*, 88.
- (31) Latif Abuhijleh, A.; Woods, C. J. *Inorg. Biochem.* **1996**, *64*, 55.
- (32) Leung, M. H. M.; Mohan, P.; Pukala, T. L.; Scanlon, D. B.; Lincoln, S. F.; Kee, T. W. *Aust. J. Chem.* **2012**, *65*, 490.
- (33) Yasumatsu, N.; Yoshikawa, Y.; Adachi, Y.; Sakurai, H. *Bioorg Med Chem* **2007**, *15*, 4917.
- (34) Sharma, S.; Athar, F.; Maurya, M. R.; Azam, A. *Eur J Med Chem* **2005**, *40*, 1414.
- (35) Sylla-Iyarreta Veitia, M.; Dumas, F.; Morgant, G.; Sorenson, J. R.; Frapart, Y.; Tomas, A. *Biochimie* **2009**, *91*, 1286.
- (36) Rivero-Müller, A.; De Vizcaya-Ruiz, A.; Plant, N.; Ruiz, L.; Dobrota, M. *Chem. Biol. Interact.* **2007**, *165*, 189.
- (37) Latif Abu Hijleh, A. *Polyhedron* **1989**, *8*, 2777.
- (38) Suksrichavalit, T.; Prachayasittikul, S.; Nantasenamat, C.; Isarankura-Na-Ayudhya, C.; Prachayasittikul, V. *Eur J Med Chem* **2009**, *44*, 3259.
- (39) Dudev, T.; Lim, C. J. *Am. Chem. Soc.* **2006**, *128*, 1553.
- (40) Collins, M.; Ewing, D.; Mackenzie, G.; Sinn, E.; Sandbhor, U.; Padhye, S.; Padhye, S. *Inorg. Chem. Commun.* **2000**, *3*, 453.
- (41) Kaluđerović, M. R.; Gómez-Ruiz, S.; Gallego, B.; Hey-Hawkins, E.; Paschke, R.; Kaluđerović, G. N. *Eur. J. Med. Chem* **2010**, *45*, 519.
- (42) Deacon, G. B.; Phillips, R. J. *Coord. Chem. Rev.* **1980**, *33*, 227.
- (43) Chen, X.-M.; Xu, Z.-T.; Yu, X.-L.; Mak, T. C. W. *Polyhedron* **1994**, *13*, 2079.
- (44) Ye, B.-H.; Li, X.-Y.; Williams, I. D.; Chen, X.-M. *Inorg. Chem.* **2002**, *41*, 6426.
- (45) Hagadorn, J. R.; Que, L.; Tolman, W. B. *Inorg. Chem.* **2000**, *39*, 6086.
- (46) Colacio, E.; Domínguez-Vera, J. M.; Ghazi, M.; Kivekäs, R.; Klinga, M.; Moreno, J. M. *Eur. J. Inorg. Chem.* **1999**, *1999*, 441.
- (47) Devereux, M.; McCann, M.; Casey, M. T.; Curran, M.; Ferguson, G.; Cardin, C.; Convery, M.; Quillet, V. *J. Chem. Soc., Dalton Trans.* **1995**, 771.
- (48) Zeleňák, V.; Vargová, Z.; Györyová, K. *Spectrochim Acta A Mol Biomol Spectrosc* **2007**, *66*, 262.
- (49) Abuhijleh, A. L. *Inorg. Chem. Commun.* **2011**, *14*, 759.
- (50) Abuhijleh, A. L. *J. Mol. Struct.* **2010**, *980*, 201.
- (51) Gumilar, F.; Agotegaray, M.; Bras, C.; Gandini, N. A.; Minetti, A.; Quinzani, O. *Eur. J. Pharmacol.* **2012**, *675*, 32.
- (52) Valko, M.; Leibfritz, D.; Moncol, J.; Cronin, M. T. D.; Mazur, M.; Telser, J. *INT J BIOCHEM CELL B* **2007**, *39*, 44.
- (53) Haas, H. *Am. J. Med* **1983**, *75*, 1.
- (54) Dimiza, F.; Perdih, F.; Tangoulis, V.; Turel, I.; Kessissoglou, D. P.; Psomas, G. *J. Inorg. Biochem.* **2011**, *105*, 476.
- (55) Amborabé, B.-E.; Fleurat-Lessard, P.; Chollet, J.-F.; Roblin, G. *Plant Physiol. Biochem.* **2002**, *40*, 1051.



- (56) Kantouch, A.; El-Sayed, A. A.; Salama, M.; El-Kheir, A. A.; Mowafi, S. *Int. J. Biol. Macromol.* **2013**, *62*, 603.
- (57) O'Connor, M. Theses, Ph.D, Dublin Institute of Technology, 2007.
- (58) Dimiza, F.; Papadopoulos, A. N.; Tangoulis, V.; Psycharis, V.; Raptopoulou, C. P.; Kessissoglou, D. P.; Psomas, G. *J. Inorg. Biochem.* **2012**, *107*, 54.
- (59) Solomons, T. W. G.; Fryhle, C.; Snyder, S. *Organic Chemistry, 11th Edition*, 2012.
- (60) Nakamoto, K. *Infrared and Raman Spectra of Inorganic and Coordination Compounds, Applications in Coordination, Organometallic, and Bioinorganic Chemistry*; Wiley, 2009.
- (61) Allen, S. E.; Walvoord, R. R.; Padilla-Salinas, R.; Kozlowski, M. C. *Chem. Rev.* **2013**, *113*, 6234.
- (62) Banu, K. S.; Chattopadhyay, T.; Banerjee, A.; Bhattacharya, S.; Zangrando, E.; Das, D. *J. Mol. Catal. A: Chem.* **2009**, *310*, 34.
- (63) Lippard, S. J.; Berg, J. M. *Principles of Bioinorganic Chemistry*; University Science Books, 1994.
- (64) Selmeczi, K.; Réglér, M.; Giorgi, M.; Speier, G. *Coord. Chem. Rev.* **2003**, *245*, 191.
- (65) Olmedo, P.; Hernández, A. F.; Pla, A.; Femia, P.; Navas-Acien, A.; Gil, F. *Food Chem. Toxicol.*
- (66) Rubino, J. T.; Franz, K. J. *J. Inorg. Biochem.* **2012**, *107*, 129.
- (67) Koval, I. A.; Gamez, P.; Belle, C.; Selmeczi, K.; Reedijk, J. *Chem. Soc. Rev.* **2006**, *35*, 814.
- (68) Crichton, R. *Biological Inorganic Chemistry: A New Introduction to molecular structure and function*; Elsevier Science, 2012.
- (69) Hough, M. A.; Hasnain, S. S. *Structure* **2003**, *11*, 937.
- (70) Bertini, I.; Manganl, S.; Viezzoli, M. S. In *Adv. Inorg. Chem.*; Sykes, A. G., Ed.; Academic Press, 1998; Vol. Volume 45.
- (71) Tainer, J. A.; Getzoff, E. D.; Richardson, J. S.; Richardson, D. C. *Nature* **1983**, *306*, 284.
- (72) Messerschmidt, A. In *Comprehensive Natural Products II*; Liu, H.-W., Mander, L., Eds.; Elsevier: Oxford, 2010.
- (73) Hashimoto, S.; Ono, K.; Takeuchi, H. *Journal of Raman Spectroscopy* **1998**, *29*, 969.
- (74) Itoh, S. In *Comprehensive Coordination Chemistry II*; McCleverty, J. A., Meyer, T. J., Eds.; Pergamon: Oxford, 2003.
- (75) Festa, R. A.; Thiele, D. J. *Current Biology* **2011**, *21*, R877.
- (76) Olmazu, C.; Puiu, M.; Babaligea, I.; Răducan, A.; Oancea, D. *Appl. Catal. A* **2012**, *447–448*, 74.
- (77) Kaizer, J.; Baráth, G.; Csonka, R.; Speier, G.; Korecz, L.; Rockenbauer, A.; Párkányi, L. *J. Inorg. Biochem.* **2008**, *102*, 773.
- (78) Panja, A. *Polyhedron* **2012**, *43*, 22.
- (79) Eicken, C.; Zippel, F.; Büldt-Karentzopoulos, K.; Krebs, B. *FEBS Lett.* **1998**, *436*, 293.
- (80) Fairhead, M.; Thöny-Meyer, L. *N. Biotechnol* **2012**, *29*, 183.
- (81) Pal, K.; Paulson, A. T.; Rousseau, D. In *Handbook of Biopolymers and Biodegradable Plastics*; Ebnesajjad, S., Ed.; William Andrew Publishing: Boston, 2013.

- (82) Kaizer, J.; Csonka, R.; Speier, G. *J. Mol. Catal. A: Chem.* **2002**, *180*, 91.
- (83) Horváth, T.; Kaizer, J.; Speier, G. *J. Mol. Catal. A: Chem.* **2004**, *215*, 9.
- (84) Hassanein, M.; El-Khalafy, S.; Shendy, S. *Catal. Commun.* **2013**, *40*, 125.
- (85) Tyagi, N.; Mathur, P. *Spectrochim Acta A Mol Biomol Spectrosc* **2012**, *96*, 759.
- (86) Sylvestre, S.; Sebastian, S.; Oudayakumar, K.; Jayavarthanam, T.; Sundaraganesan, N. *Spectrochim Acta A Mol Biomol Spectrosc* **2012**, *96*, 401.
- (87) Latif Abuhijleh, A. *Polyhedron* **1996**, *15*, 285.
- (88) Hu, L.; Yuan, Y.; Zhang, L.; Zhao, J.; Majeed, S.; Xu, G. *Anal. Chim. Acta* **2013**, *762*, 83.
- (89) Zhang, K.; Cai, R.; Chen, D.; Mao, L. *Anal. Chim. Acta* **2000**, *413*, 109.
- (90) Liu, H.; Wang, Z.; Liu, Y.; Xiao, J.; Wang, C. *Thermochim. Acta* **2006**, *443*, 173.
- (91) Sorenson, J. R. *J. Med. Chem.* **1976**, *19*, 135.
- (92) Fersht, A. R.; Kirby, A. J. *J. Am. Chem. Soc.* **1967**, *89*, 4857.
- (93) Hassanein, M.; Abdo, M.; Gerges, S.; El-Khalafy, S. *J. Mol. Catal. A: Chem.* **2008**, *287*, 53.
- (94) Monzani, E.; Quinti, L.; Perotti, A.; Casella, L.; Gullotti, M.; Randaccio, L.; Geremia, S.; Nardin, G.; Faleschini, P.; Tabbi, G. *Inorg. Chem.* **1998**, *37*, 553.
- (95) Mukherjee, C.; Weyhermüller, T.; Bothe, E.; Chaudhuri, P. *Comptes Rendus Chimie* **2007**, *10*, 313.
- (96) Abuhijleh, A. L. *J. Inorg. Biochem.* **1994**, *55*, 255.
- (97) Valderrama-Negrón, A. C.; Alves, W. A.; Cruz, Á. S.; Rogero, S. O.; de Oliveira Silva, D. *Inorg. Chim. Acta* **2011**, *367*, 85.
- (98) Calabrese, I.; Cavallaro, G.; Scialabba, C.; Licciardi, M.; Merli, M.; Sciascia, L.; Turco Liveri, M. L. *Int. J. Pharm.* **2013**, *457*, 224.
- (99) Abuhijleh, A. L.; Woods, C. *Inorg. Chim. Acta* **1992**, *194*, 9.
- (100) Abuhijleh, A. L.; Woods, C. *Inorg. Chem. Commun.* **2001**, *4*, 119.
- (101) Guha, A.; Chattopadhyay, T.; Paul, N. D.; Mukherjee, M.; Goswami, S.; Mondal, T. K.; Zangrando, E.; Das, D. *Inorg Chem* **2012**, *51*, 8750.
- (102) Magdalou, J.; Hochman, Y.; Zakim, D. *J Biol Inorg Chem* **1982**, *257*, 13624.
- (103) Siegbahn, P. M. *J Biol Inorg Chem* **2004**, *9*, 577.
- (104) Banu, K. S.; Mukherjee, M.; Guha, A.; Bhattacharya, S.; Zangrando, E.; Das, D. *Polyhedron* **2012**, *45*, 245.
- (105) Banu, K. S.; Chattopadhyay, T.; Banerjee, A.; Bhattacharya, S.; Suresh, E.; Nethaji, M.; Zangrando, E.; Das, D. *Inorg. Chem.* **2008**, *47*, 7083.
- (106) Mouadili, A.; Attayibat, A.; Kadiri, S. E.; Radi, S.; Touzani, R. *Appl. Catal. A* **2013**, *454*, 93.
- (107) Le Roes-Hill, M.; Goodwin, C.; Burton, S. *Trends Biotechnol.* **2009**, *27*, 248.

## 5. APPENDICES

### 5.1. APPENDIX A: Crystal data and structure of [Cu(sal)<sub>2</sub>(pz)<sub>2</sub>] (1).

**Table I.** Crystal data and structure refinement for **1**.

Empirical formula	C <sub>20</sub> H <sub>18</sub> Cu N <sub>4</sub> O <sub>6</sub>	
Formula weight	473.92	
Temperature	293(1) K	
Wavelength	0.71073 Å	
Crystal system	Monoclinic	
Space group	P2(1)/n	
Unit cell dimensions	a = 5.1347(5) Å	α = 90°.
	b = 20.532(2) Å	β = 104.510(1)°.
	c = 9.6258(8) Å	γ = 90°.
Volume	982.4(2) Å <sup>3</sup>	
Z	2	
Density (calculated)	1.602 Mg/m <sup>3</sup>	
Absorption coefficient	1.159 mm <sup>-1</sup>	
F(000)	486	
Crystal size	0.34 x 0.12 x 0.08 mm <sup>3</sup>	
Theta range for data collection	2.95 to 28.00°.	
Index ranges	-6 ≤ h ≤ 6, -27 ≤ k ≤ 26, -12 ≤ l ≤ 12	
Reflections collected	11271	
Independent reflections	2341 [R(int) = 0.0253]	
Completeness to theta = 28.00°	98.9 %	
Absorption correction	None	
Refinement method	Full-matrix least-squares on F <sup>2</sup>	
Data / restraints / parameters	2341 / 0 / 142	
Goodness-of-fit on F <sup>2</sup>	1.236	
Final R indices [I > 2σ(I)]	R1 = 0.0518, wR2 = 0.1173	
R indices (all data)	R1 = 0.0556, wR2 = 0.1193	
Largest diff. peak and hole	0.384 and -0.301 e.Å <sup>-3</sup>	

**Table II.** Atomic coordinates ( $\times 10^4$ ) and equivalent isotropic displacement parameters ( $\text{\AA}^2 \times 10^3$ )for **1**.  $U(\text{eq})$  is defined as one third of the trace of the orthogonalized  $U^{ij}$  tensor.

	x	y	z	$U(\text{eq})$
C(1)	3999(5)	6454(1)	8713(3)	34(1)
C(2)	5599(5)	6537(1)	7746(3)	31(1)
C(3)	7226(7)	7088(2)	7879(4)	46(1)
C(4)	7282(8)	7547(2)	8916(4)	57(1)
C(5)	5666(8)	7464(2)	9854(4)	54(1)
C(6)	4050(7)	6928(2)	9761(3)	46(1)
C(7)	5682(5)	6053(1)	6605(3)	32(1)
C(8)	-1482(6)	6018(2)	2633(4)	48(1)
C(9)	-542(7)	5816(2)	1497(3)	50(1)
C(10)	1675(6)	5441(2)	2088(3)	44(1)
Cu(1)	5000	5000	5000	32(1)
N(1)	2109(5)	5413(1)	3517(2)	36(1)
N(2)	132(5)	5773(1)	3821(3)	38(1)
O(1)	4087(4)	5555(1)	6489(2)	37(1)
O(2)	7208(5)	6124(1)	5810(2)	47(1)
O(3)	2411(5)	5928(1)	8712(2)	51(1)

**Table III.** Bond lengths [ $\text{\AA}$ ] and angles [ $^\circ$ ] for **1**.

---

C(1)-O(3)	1.353(4)
C(1)-C(6)	1.396(4)
C(1)-C(2)	1.398(4)
C(2)-C(3)	1.393(4)
C(2)-C(7)	1.489(3)
C(3)-C(4)	1.367(4)
C(3)-H(3)	0.9300
C(4)-C(5)	1.381(5)
C(4)-H(4)	0.9300
C(5)-C(6)	1.369(5)
C(5)-H(5)	0.9300
C(6)-H(6)	0.9300
C(7)-O(2)	1.233(3)
C(7)-O(1)	1.298(3)
C(8)-N(2)	1.331(4)
C(8)-C(9)	1.365(4)
C(8)-H(8)	0.9361
C(9)-C(10)	1.374(4)
C(9)-H(9)	0.9119
C(10)-N(1)	1.339(3)
C(10)-H(10)	0.9113
Cu(1)-N(1)	1.974(2)
Cu(1)-N(1)#1	1.974(2)
Cu(1)-O(1)	1.9766(17)
Cu(1)-O(1)#1	1.9766(17)

N(1)-N(2)	1.346(3)
N(2)-H(1N2)	0.8540
O(3)-H(1O3)	0.7889
O(3)-C(1)-C(6)	117.3(2)
O(3)-C(1)-C(2)	123.4(2)
C(6)-C(1)-C(2)	119.3(3)
C(3)-C(2)-C(1)	118.4(2)
C(3)-C(2)-C(7)	118.8(2)
C(1)-C(2)-C(7)	122.7(2)
C(4)-C(3)-C(2)	121.9(3)
C(4)-C(3)-H(3)	119.0
C(2)-C(3)-H(3)	119.0
C(3)-C(4)-C(5)	119.1(3)
C(3)-C(4)-H(4)	120.4
C(5)-C(4)-H(4)	120.4
C(6)-C(5)-C(4)	120.6(3)
C(6)-C(5)-H(5)	119.7
C(4)-C(5)-H(5)	119.7
C(5)-C(6)-C(1)	120.6(3)
C(5)-C(6)-H(6)	119.7
C(1)-C(6)-H(6)	119.7
O(2)-C(7)-O(1)	121.6(2)
O(2)-C(7)-C(2)	121.3(3)
O(1)-C(7)-C(2)	117.1(2)
N(2)-C(8)-C(9)	107.8(3)
N(2)-C(8)-H(8)	121.9
C(9)-C(8)-H(8)	130.3

C(8)-C(9)-C(10)	105.1(3)
C(8)-C(9)-H(9)	128.8
C(10)-C(9)-H(9)	125.8
N(1)-C(10)-C(9)	110.9(3)
N(1)-C(10)-H(10)	121.8
C(9)-C(10)-H(10)	127.3
N(1)-Cu(1)-N(1)#1	180.000(1)
N(1)-Cu(1)-O(1)	90.27(9)
N(1)#1-Cu(1)-O(1)	89.73(9)
N(1)-Cu(1)-O(1)#1	89.73(9)
N(1)#1-Cu(1)-O(1)#1	90.27(9)
O(1)-Cu(1)-O(1)#1	180.000(1)
C(10)-N(1)-N(2)	105.0(2)
C(10)-N(1)-Cu(1)	131.5(2)
N(2)-N(1)-Cu(1)	123.39(18)
C(8)-N(2)-N(1)	111.2(2)
C(8)-N(2)-H(1N2)	120.8
N(1)-N(2)-H(1N2)	127.8
C(7)-O(1)-Cu(1)	104.94(15)
C(1)-O(3)-H(1O3)	104.7

---

Symmetry transformations used to generate equivalent atoms:

#1 -x+1,-y+1,-z+1

**Table IV.** Anisotropic displacement parameters ( $\text{\AA}^2 \times 10^3$ ) for **1**. The anisotropicdisplacement factor exponent takes the form:  $-2\pi^2 [ h^2 a^{*2} U^{11} + \dots + 2 h k a^* b^* U^{12} ]$ 

	$U^{11}$	$U^{22}$	$U^{33}$	$U^{23}$	$U^{13}$	$U^{12}$
C(1)	36(1)	39(1)	29(1)	-3(1)	12(1)	4(1)
C(2)	37(1)	33(1)	25(1)	-2(1)	11(1)	9(1)
C(3)	56(2)	41(2)	49(2)	-5(1)	29(2)	-1(1)
C(4)	65(2)	43(2)	71(2)	-18(2)	32(2)	-13(2)
C(5)	63(2)	52(2)	55(2)	-25(2)	28(2)	-4(2)
C(6)	51(2)	56(2)	39(2)	-13(1)	24(1)	2(2)
C(7)	39(1)	34(1)	25(1)	-2(1)	10(1)	8(1)
C(8)	40(2)	56(2)	49(2)	4(2)	13(1)	9(1)
C(9)	51(2)	63(2)	34(2)	6(1)	9(1)	6(2)
C(10)	47(2)	56(2)	29(1)	-4(1)	13(1)	4(1)
Cu(1)	38(1)	36(1)	25(1)	-7(1)	13(1)	3(1)
N(1)	38(1)	42(1)	30(1)	-4(1)	13(1)	5(1)
N(2)	40(1)	43(1)	36(1)	-3(1)	19(1)	2(1)
O(1)	44(1)	40(1)	30(1)	-10(1)	15(1)	2(1)
O(2)	60(1)	51(1)	39(1)	-6(1)	31(1)	3(1)
O(3)	65(2)	55(1)	44(1)	-15(1)	34(1)	-16(1)



**Table V.** Hydrogen coordinates ( $\times 10^4$ ) and isotropic displacement parameters ( $\text{\AA}^2 \times 10^3$ )for **1**.

	x	y	z	U(eq)
H(3)	8304	7146	7243	55
H(4)	8394	7909	8989	69
H(5)	5677	7777	10555	65
H(6)	2975	6878	10401	55
H(8)	-2991	6269	2657	72
H(9)	-1113	5933	555	75
H(10)	2765	5233	1616	65
H(1N2)	-209	5829	4637	57
H(1O3)	2402	5744	7991	76

**Table VI.** Hydrogen bonds for **1** [ $\text{\AA}$  and  $^\circ$ ].

D-H...A	d(D-H)	d(H...A)	d(D...A)	$\angle(\text{DHA})$
N(2)-H(1N2)...O(2)#2	0.85	2.04	2.806(3)	149.5
O(3)-H(1O3)...O(1)	0.79	1.90	2.614(3)	149.7

Symmetry transformations used to generate equivalent atoms:

#1  $-x+1, -y+1, -z+1$  #2  $x-1, y, z$

## 5.2. APPENDIX B: Crystal data and structure of $[\text{Cu}(\text{nap})_2(\text{pz})_4]$ (**2**).

Table I. Crystal data and structure refinement for **2**.

Empirical formula	C <sub>40</sub> H <sub>42</sub> Cu N <sub>8</sub> O <sub>6</sub>	
Formula weight	794.36	
Temperature	293(1) K	
Wavelength	0.71073 $\text{\AA}$	
Crystal system	Monoclinic	
Space group	P2(1)	
Unit cell dimensions	$a = 8.630(2) \text{\AA}$	$\alpha = 90^\circ$ .
	$b = 25.675(5) \text{\AA}$	$\beta = 94.071(3)^\circ$ .
	$c = 8.782(2) \text{\AA}$	$\gamma = 90^\circ$ .
Volume	$1941.0(6) \text{\AA}^3$	
Z	2	
Density (calculated)	1.359 $\text{Mg/m}^3$	
Absorption coefficient	0.620 $\text{mm}^{-1}$	
F(000)	830	

Crystal size	0.28 x 0.26 x 0.21 mm <sup>3</sup>
Theta range for data collection	2.33 to 27.00°.
Index ranges	-11<=h<=11, -32<=k<=32, -11<=l<=11
Reflections collected	21581
Independent reflections	8348 [R(int) = 0.0280]
Completeness to theta = 27.00°	99.4 %
Absorption correction	None
Refinement method	Full-matrix least-squares on F <sup>2</sup>
Data / restraints / parameters	8348 / 5 / 512
Goodness-of-fit on F <sup>2</sup>	1.037
Final R indices [I>2sigma(I)]	R1 = 0.0445, wR2 = 0.1153
R indices (all data)	R1 = 0.0542, wR2 = 0.1207
Absolute structure parameter	0.004(10)
Largest diff. peak and hole	0.346 and -0.263 e.Å <sup>-3</sup>

**Table II.** Atomic coordinates ( x 10<sup>4</sup>) and equivalent isotropic displacement parameters (Å<sup>2</sup>x 10<sup>3</sup>)

for **2**. U(eq) is defined as one third of the trace of the orthogonalized U<sup>ij</sup> tensor.

	x	y	z	U(eq)
C(1)	2066(4)	3740(1)	11015(4)	64(1)
C(2)	1191(4)	3220(1)	10771(4)	72(1)
C(3)	2253(6)	2763(2)	11027(6)	104(1)
C(4)	-174(4)	3230(1)	11771(4)	63(1)
C(5)	-1598(4)	3433(1)	11209(4)	74(1)
C(6)	-2830(4)	3478(2)	12088(4)	75(1)

C(7)	-2708(4)	3323(1)	13624(4)	62(1)
C(8)	-3962(4)	3367(1)	14572(4)	69(1)
C(9)	-3769(5)	3223(1)	16067(4)	69(1)
C(10)	-2337(4)	3028(1)	16678(4)	75(1)
C(11)	-1117(4)	2974(1)	15785(4)	73(1)
C(12)	-1270(4)	3119(1)	14228(4)	61(1)
C(13)	-15(4)	3073(1)	13265(4)	65(1)
C(14)	-6414(6)	3396(2)	16491(6)	110(2)
C(15)	2121(4)	6293(1)	8618(4)	71(1)
C(16)	2891(3)	6823(1)	8412(3)	60(1)
C(17)	3178(5)	7098(2)	9948(5)	96(1)
C(18)	4354(3)	6766(1)	7563(3)	56(1)
C(19)	4371(4)	6924(1)	6069(3)	59(1)
C(20)	5685(4)	6867(1)	5239(4)	58(1)
C(21)	5707(4)	7012(1)	3682(4)	73(1)
C(22)	6997(5)	6955(1)	2913(4)	76(1)
C(23)	8344(5)	6746(1)	3634(4)	71(1)
C(24)	8391(4)	6592(1)	5120(4)	65(1)
C(25)	7049(4)	6648(1)	5958(4)	58(1)
C(26)	7023(3)	6492(1)	7493(4)	65(1)
C(27)	5717(3)	6549(1)	8258(3)	62(1)
C(28)	10955(5)	6492(3)	3376(7)	125(2)

C(29)	4348(5)	4972(2)	14143(4)	92(1)
C(30)	4479(5)	5479(2)	13950(5)	89(1)
C(31)	3883(4)	5569(1)	12458(4)	73(1)
C(32)	6433(4)	5042(2)	7767(4)	80(1)
C(33)	6455(4)	4536(2)	8047(5)	87(1)
C(34)	5125(4)	4425(1)	8757(4)	75(1)
C(35)	21(5)	4479(2)	5670(5)	100(1)
C(36)	64(6)	4991(2)	5394(4)	106(1)
C(37)	740(4)	5210(1)	6641(4)	74(1)
C(38)	-1918(4)	5547(2)	11300(5)	88(1)
C(39)	-2042(3)	5051(2)	11699(4)	78(1)
C(40)	-725(4)	4812(1)	11249(4)	69(1)
Cu(1)	2242(1)	5000(1)	9775(1)	65(1)
N(1)	3363(3)	5142(1)	11829(3)	60(1)
N(2)	3659(3)	4766(1)	12851(3)	72(1)
N(3)	4302(3)	4854(1)	8917(3)	60(1)
N(4)	5122(3)	5230(1)	8292(3)	68(1)
N(5)	1141(3)	4872(1)	7687(3)	64(1)
N(6)	705(4)	4422(1)	7104(4)	89(1)
N(7)	179(3)	5150(1)	10618(3)	62(1)
N(8)	-554(4)	5594(1)	10614(5)	89(1)
O(1)	1762(4)	4092(1)	10115(4)	108(1)

O(2)	3014(4)	3781(1)	12138(4)	116(1)
O(3)	-4897(4)	3252(1)	17083(3)	88(1)
O(4)	2857(3)	5918(1)	9128(3)	79(1)
O(5)	807(5)	6274(2)	8313(11)	267(5)
O(6)	9567(3)	6721(1)	2722(4)	93(1)

---

**Table III.** Bond lengths [ $\text{\AA}$ ] and angles [ $^\circ$ ] for **2**.

---

C(1)-O(1)	1.219(4)
C(1)-O(2)	1.241(5)
C(1)-C(2)	1.540(5)
C(2)-C(3)	1.497(5)
C(2)-C(4)	1.519(5)
C(2)-H(2)	0.9800
C(3)-H(3A)	0.9600
C(3)-H(3B)	0.9600
C(3)-H(3C)	0.9600
C(4)-C(13)	1.370(5)
C(4)-C(5)	1.392(5)
C(5)-C(6)	1.363(5)
C(5)-H(5)	0.9300
C(6)-C(7)	1.402(5)

C(6)-H(6)	0.9300
C(7)-C(12)	1.415(5)
C(7)-C(8)	1.416(5)
C(8)-C(9)	1.362(5)
C(8)-H(8)	0.9300
C(9)-O(3)	1.369(4)
C(9)-C(10)	1.404(5)
C(10)-C(11)	1.363(5)
C(10)-H(10)	0.9300
C(11)-C(12)	1.414(5)
C(11)-H(11)	0.9300
C(12)-C(13)	1.426(5)
C(13)-H(13)	0.9300
C(14)-O(3)	1.422(6)
C(14)-H(14A)	0.9600
C(14)-H(14B)	0.9600
C(14)-H(14C)	0.9600
C(15)-O(5)	1.148(5)
C(15)-O(4)	1.220(4)
C(15)-C(16)	1.531(5)
C(16)-C(18)	1.519(4)
C(16)-C(17)	1.527(5)

C(16)-H(16)	0.9800
C(17)-H(17A)	0.9600
C(17)-H(17B)	0.9600
C(17)-H(17C)	0.9600
C(18)-C(19)	1.375(4)
C(18)-C(27)	1.402(4)
C(19)-C(20)	1.399(5)
C(19)-H(19)	0.9300
C(20)-C(25)	1.412(4)
C(20)-C(21)	1.419(4)
C(21)-C(22)	1.351(5)
C(21)-H(21)	0.9300
C(22)-C(23)	1.392(5)
C(22)-H(22)	0.9300
C(23)-C(24)	1.361(5)
C(23)-O(6)	1.370(5)
C(24)-C(25)	1.423(5)
C(24)-H(24)	0.9300
C(25)-C(26)	1.408(4)
C(26)-C(27)	1.361(4)
C(26)-H(26)	0.9300
C(27)-H(27)	0.9300



C(28)-O(6)	1.420(6)
C(28)-H(28A)	0.9600
C(28)-H(28B)	0.9600
C(28)-H(28C)	0.9600
C(29)-C(30)	1.316(7)
C(29)-N(2)	1.351(5)
C(29)-H(29)	0.9300
C(30)-C(31)	1.393(5)
C(30)-H(30)	0.9300
C(31)-N(1)	1.294(4)
C(31)-H(31)	0.9300
C(32)-C(33)	1.322(7)
C(32)-N(4)	1.341(4)
C(32)-H(32)	0.9300
C(33)-C(34)	1.375(5)
C(33)-H(33)	0.9300
C(34)-N(3)	1.323(4)
C(34)-H(34)	0.9300
C(35)-C(36)	1.338(8)
C(35)-N(6)	1.360(6)
C(35)-H(35)	0.9300
C(36)-C(37)	1.329(5)

C(36)-H(36)	0.9300
C(37)-N(5)	1.292(4)
C(37)-H(37)	0.9300
C(38)-C(39)	1.327(7)
C(38)-N(8)	1.365(5)
C(38)-H(38)	0.9300
C(39)-C(40)	1.374(5)
C(39)-H(39)	0.9300
C(40)-N(7)	1.316(4)
C(40)-H(40)	0.9300
Cu(1)-N(7)	2.014(2)
Cu(1)-N(3)	2.014(2)
Cu(1)-N(1)	2.019(2)
Cu(1)-N(5)	2.031(2)
Cu(1)-O(1)	2.389(3)
Cu(1)-O(4)	2.490(2)
N(1)-N(2)	1.330(4)
N(2)-H(2N)	0.886(10)
N(3)-N(4)	1.338(4)
N(4)-H(4N)	0.890(10)
N(5)-N(6)	1.309(4)
N(6)-H(6N)	0.899(10)

N(7)-N(8)	1.305(4)
N(8)-H(8N)	0.889(10)
O(1)-H(6N)	2.32(5)
O(2)-H(2N)	1.81(2)
O(4)-H(4N)	2.04(3)
O(5)-H(8N)	2.14(3)
O(1)-C(1)-O(2)	123.5(3)
O(1)-C(1)-C(2)	118.2(3)
O(2)-C(1)-C(2)	118.3(3)
C(3)-C(2)-C(4)	114.7(3)
C(3)-C(2)-C(1)	111.7(3)
C(4)-C(2)-C(1)	107.3(3)
C(3)-C(2)-H(2)	107.6
C(4)-C(2)-H(2)	107.6
C(1)-C(2)-H(2)	107.6
C(2)-C(3)-H(3A)	109.5
C(2)-C(3)-H(3B)	109.5
H(3A)-C(3)-H(3B)	109.5
C(2)-C(3)-H(3C)	109.5
H(3A)-C(3)-H(3C)	109.5
H(3B)-C(3)-H(3C)	109.5
C(13)-C(4)-C(5)	118.4(3)

C(13)-C(4)-C(2)	121.3(3)
C(5)-C(4)-C(2)	120.1(3)
C(6)-C(5)-C(4)	122.3(3)
C(6)-C(5)-H(5)	118.8
C(4)-C(5)-H(5)	118.8
C(5)-C(6)-C(7)	120.8(3)
C(5)-C(6)-H(6)	119.6
C(7)-C(6)-H(6)	119.6
C(6)-C(7)-C(12)	118.0(3)
C(6)-C(7)-C(8)	122.3(3)
C(12)-C(7)-C(8)	119.6(3)
C(9)-C(8)-C(7)	119.9(3)
C(9)-C(8)-H(8)	120.0
C(7)-C(8)-H(8)	120.0
C(8)-C(9)-O(3)	124.7(4)
C(8)-C(9)-C(10)	120.6(3)
O(3)-C(9)-C(10)	114.7(3)
C(11)-C(10)-C(9)	120.7(3)
C(11)-C(10)-H(10)	119.6
C(9)-C(10)-H(10)	119.6
C(10)-C(11)-C(12)	120.4(3)
C(10)-C(11)-H(11)	119.8

C(12)-C(11)-H(11)	119.8
C(11)-C(12)-C(7)	118.7(3)
C(11)-C(12)-C(13)	121.9(3)
C(7)-C(12)-C(13)	119.4(3)
C(4)-C(13)-C(12)	121.0(3)
C(4)-C(13)-H(13)	119.5
C(12)-C(13)-H(13)	119.5
O(3)-C(14)-H(14A)	109.5
O(3)-C(14)-H(14B)	109.5
H(14A)-C(14)-H(14B)	109.5
O(3)-C(14)-H(14C)	109.5
H(14A)-C(14)-H(14C)	109.5
H(14B)-C(14)-H(14C)	109.5
O(5)-C(15)-O(4)	122.1(4)
O(5)-C(15)-C(16)	116.1(3)
O(4)-C(15)-C(16)	121.7(3)
C(18)-C(16)-C(17)	112.9(3)
C(18)-C(16)-C(15)	110.8(2)
C(17)-C(16)-C(15)	110.6(3)
C(18)-C(16)-H(16)	107.4
C(17)-C(16)-H(16)	107.4
C(15)-C(16)-H(16)	107.4

C(16)-C(17)-H(17A)	109.5
C(16)-C(17)-H(17B)	109.5
H(17A)-C(17)-H(17B)	109.5
C(16)-C(17)-H(17C)	109.5
H(17A)-C(17)-H(17C)	109.5
H(17B)-C(17)-H(17C)	109.5
C(19)-C(18)-C(27)	117.9(3)
C(19)-C(18)-C(16)	120.4(2)
C(27)-C(18)-C(16)	121.7(3)
C(18)-C(19)-C(20)	122.0(3)
C(18)-C(19)-H(19)	119.0
C(20)-C(19)-H(19)	119.0
C(19)-C(20)-C(25)	119.3(3)
C(19)-C(20)-C(21)	122.8(3)
C(25)-C(20)-C(21)	117.9(3)
C(22)-C(21)-C(20)	121.4(3)
C(22)-C(21)-H(21)	119.3
C(20)-C(21)-H(21)	119.3
C(21)-C(22)-C(23)	120.4(3)
C(21)-C(22)-H(22)	119.8
C(23)-C(22)-H(22)	119.8
C(24)-C(23)-O(6)	125.1(4)

C(24)-C(23)-C(22)	121.0(3)
O(6)-C(23)-C(22)	113.9(3)
C(23)-C(24)-C(25)	119.8(3)
C(23)-C(24)-H(24)	120.1
C(25)-C(24)-H(24)	120.1
C(26)-C(25)-C(20)	118.2(3)
C(26)-C(25)-C(24)	122.3(3)
C(20)-C(25)-C(24)	119.5(3)
C(27)-C(26)-C(25)	120.9(3)
C(27)-C(26)-H(26)	119.6
C(25)-C(26)-H(26)	119.6
C(26)-C(27)-C(18)	121.7(3)
C(26)-C(27)-H(27)	119.1
C(18)-C(27)-H(27)	119.1
O(6)-C(28)-H(28A)	109.5
O(6)-C(28)-H(28B)	109.5
H(28A)-C(28)-H(28B)	109.5
O(6)-C(28)-H(28C)	109.5
H(28A)-C(28)-H(28C)	109.5
H(28B)-C(28)-H(28C)	109.5
C(30)-C(29)-N(2)	108.5(3)
C(30)-C(29)-H(29)	125.8

N(2)-C(29)-H(29)	125.8
C(29)-C(30)-C(31)	104.8(3)
C(29)-C(30)-H(30)	127.6
C(31)-C(30)-H(30)	127.6
N(1)-C(31)-C(30)	110.7(3)
N(1)-C(31)-H(31)	124.7
C(30)-C(31)-H(31)	124.7
C(33)-C(32)-N(4)	107.0(4)
C(33)-C(32)-H(32)	126.5
N(4)-C(32)-H(32)	126.5
C(32)-C(33)-C(34)	106.6(3)
C(32)-C(33)-H(33)	126.7
C(34)-C(33)-H(33)	126.7
N(3)-C(34)-C(33)	110.4(3)
N(3)-C(34)-H(34)	124.8
C(33)-C(34)-H(34)	124.8
C(36)-C(35)-N(6)	104.9(3)
C(36)-C(35)-H(35)	127.5
N(6)-C(35)-H(35)	127.5
C(37)-C(36)-C(35)	106.4(4)
C(37)-C(36)-H(36)	126.8
C(35)-C(36)-H(36)	126.8



N(5)-C(37)-C(36)	112.4(4)
N(5)-C(37)-H(37)	123.8
C(36)-C(37)-H(37)	123.8
C(39)-C(38)-N(8)	106.9(3)
C(39)-C(38)-H(38)	126.5
N(8)-C(38)-H(38)	126.5
C(38)-C(39)-C(40)	105.6(3)
C(38)-C(39)-H(39)	127.2
C(40)-C(39)-H(39)	127.2
N(7)-C(40)-C(39)	110.7(3)
N(7)-C(40)-H(40)	124.7
C(39)-C(40)-H(40)	124.7
N(7)-Cu(1)-N(3)	179.53(11)
N(7)-Cu(1)-N(1)	90.96(9)
N(3)-Cu(1)-N(1)	89.34(10)
N(7)-Cu(1)-N(5)	89.63(10)
N(3)-Cu(1)-N(5)	90.06(10)
N(1)-Cu(1)-N(5)	178.64(12)
N(7)-Cu(1)-O(1)	88.54(13)
N(3)-Cu(1)-O(1)	91.77(13)
N(1)-Cu(1)-O(1)	98.06(10)
N(5)-Cu(1)-O(1)	83.18(11)

N(7)-Cu(1)-O(4)	96.41(10)
N(3)-Cu(1)-O(4)	83.25(9)
N(1)-Cu(1)-O(4)	86.40(10)
N(5)-Cu(1)-O(4)	92.31(10)
O(1)-Cu(1)-O(4)	173.30(14)
C(31)-N(1)-N(2)	106.4(3)
C(31)-N(1)-Cu(1)	131.6(2)
N(2)-N(1)-Cu(1)	122.0(2)
N(1)-N(2)-C(29)	109.5(3)
N(1)-N(2)-H(2N)	123(3)
C(29)-N(2)-H(2N)	125(3)
C(34)-N(3)-N(4)	104.7(3)
C(34)-N(3)-Cu(1)	133.5(2)
N(4)-N(3)-Cu(1)	121.73(19)
N(3)-N(4)-C(32)	111.4(3)
N(3)-N(4)-H(4N)	116(3)
C(32)-N(4)-H(4N)	132(3)
C(37)-N(5)-N(6)	105.1(3)
C(37)-N(5)-Cu(1)	128.1(2)
N(6)-N(5)-Cu(1)	126.8(2)
N(5)-N(6)-C(35)	111.1(3)
N(5)-N(6)-H(6N)	126(4)

C(35)-N(6)-H(6N)	123(4)
N(8)-N(7)-C(40)	106.1(3)
N(8)-N(7)-Cu(1)	127.4(2)
C(40)-N(7)-Cu(1)	126.5(2)
N(7)-N(8)-C(38)	110.7(3)
N(7)-N(8)-H(8N)	124(4)
C(38)-N(8)-H(8N)	125(4)
C(1)-O(1)-H(6N)	133.2(8)
C(1)-O(1)-Cu(1)	140.8(3)
H(6N)-O(1)-Cu(1)	84.9(7)
C(1)-O(2)-H(2N)	112.0(15)
C(9)-O(3)-C(14)	117.1(3)
C(15)-O(4)-H(4N)	130.1(11)
C(15)-O(4)-Cu(1)	135.7(2)
H(4N)-O(4)-Cu(1)	80.2(10)
C(15)-O(5)-H(8N)	109.1(17)
C(23)-O(6)-C(28)	116.5(3)

---

Symmetry transformations used to generate equivalent atoms:

**Table IV.** Anisotropic displacement parameters ( $\text{\AA}^2 \times 10^3$ ) for **2**. The anisotropic displacement factor exponent takes the form:  $-2\pi^2 [ h^2 a^{*2} U^{11} + \dots + 2 h k a^* b^* U^{12} ]$

	$U^{11}$	$U^{22}$	$U^{33}$	$U^{23}$	$U^{13}$	$U^{12}$
C(1)	62(2)	59(2)	72(2)	10(1)	6(1)	8(1)
C(2)	89(2)	57(2)	71(2)	1(1)	12(2)	-5(2)
C(3)	137(4)	60(2)	119(3)	0(2)	40(3)	19(2)
C(4)	73(2)	47(1)	70(2)	0(1)	5(2)	-10(1)
C(5)	85(2)	77(2)	57(2)	10(2)	-5(2)	-7(2)
C(6)	69(2)	84(2)	71(2)	8(2)	-8(2)	7(2)
C(7)	70(2)	51(2)	63(2)	5(1)	-5(1)	-6(1)
C(8)	70(2)	59(2)	77(2)	-2(1)	3(2)	2(1)
C(9)	88(2)	50(2)	71(2)	-6(1)	11(2)	-10(2)
C(10)	92(2)	72(2)	59(2)	10(2)	-7(2)	-15(2)
C(11)	77(2)	71(2)	69(2)	15(2)	-10(2)	-10(2)
C(12)	69(2)	50(2)	62(2)	4(1)	-7(1)	-9(1)
C(13)	64(2)	57(2)	72(2)	10(1)	-4(1)	-6(1)
C(14)	100(3)	115(3)	119(4)	-2(3)	33(3)	16(3)
C(15)	49(2)	63(2)	99(2)	14(2)	-6(2)	6(1)

C(16)	63(2)	57(2)	60(2)	7(1)	-1(1)	5(1)
C(17)	111(3)	93(3)	86(3)	-24(2)	13(2)	-11(2)
C(18)	61(2)	44(1)	60(2)	6(1)	-7(1)	0(1)
C(19)	71(2)	48(1)	56(2)	4(1)	-10(1)	7(1)
C(20)	69(2)	46(1)	57(2)	4(1)	-3(1)	2(1)
C(21)	84(2)	76(2)	57(2)	8(2)	-8(2)	18(2)
C(22)	95(2)	74(2)	60(2)	5(2)	7(2)	9(2)
C(23)	82(2)	62(2)	69(2)	-2(2)	10(2)	-2(2)
C(24)	62(2)	63(2)	71(2)	5(1)	-3(1)	-2(1)
C(25)	67(2)	44(1)	61(2)	3(1)	-7(1)	-8(1)
C(26)	58(2)	71(2)	63(2)	16(1)	-13(1)	-3(1)
C(27)	65(2)	66(2)	52(2)	12(1)	-6(1)	-8(1)
C(28)	76(3)	181(6)	120(4)	15(4)	30(3)	3(3)
C(29)	108(3)	98(3)	65(2)	13(2)	-27(2)	-19(3)
C(30)	100(3)	91(3)	73(2)	-14(2)	-16(2)	-9(2)
C(31)	77(2)	68(2)	74(2)	-1(2)	-4(2)	5(2)
C(32)	56(2)	118(3)	67(2)	-15(2)	4(1)	2(2)
C(33)	62(2)	102(3)	95(3)	-26(2)	-3(2)	28(2)
C(34)	63(2)	67(2)	92(2)	-2(2)	-5(2)	15(2)
C(35)	111(3)	101(3)	86(3)	-33(2)	-8(2)	-20(3)
C(36)	133(3)	113(3)	66(2)	11(3)	-36(2)	-18(3)
C(37)	93(2)	58(2)	67(2)	6(1)	-26(2)	-11(2)

C(38)	59(2)	98(3)	106(3)	-16(2)	-12(2)	15(2)
C(39)	58(2)	109(3)	69(2)	-3(2)	9(1)	-4(2)
C(40)	64(2)	71(2)	72(2)	1(1)	14(2)	0(1)
Cu(1)	52(1)	94(1)	47(1)	0(1)	-2(1)	13(1)
N(1)	57(1)	72(2)	51(1)	0(1)	-3(1)	8(1)
N(2)	79(2)	75(2)	60(2)	4(1)	-15(1)	-8(1)
N(3)	54(1)	72(2)	55(1)	-3(1)	1(1)	7(1)
N(4)	68(2)	73(2)	63(1)	-2(1)	4(1)	8(1)
N(5)	60(1)	73(2)	56(1)	-2(1)	-3(1)	11(1)
N(6)	98(2)	82(2)	88(2)	-5(2)	8(2)	7(2)
N(7)	54(1)	79(2)	53(1)	0(1)	-3(1)	5(1)
N(8)	63(2)	88(2)	114(3)	21(2)	-6(2)	-2(2)
O(1)	126(2)	69(1)	121(2)	30(2)	-46(2)	-20(2)
O(2)	128(2)	83(2)	127(3)	27(2)	-53(2)	-13(2)
O(3)	101(2)	84(2)	83(2)	-6(1)	23(2)	-1(1)
O(4)	68(1)	60(1)	109(2)	18(1)	-4(1)	4(1)
O(5)	95(3)	112(3)	575(13)	152(5)	-107(5)	-22(2)
O(6)	89(2)	101(2)	93(2)	7(2)	30(2)	3(2)

---

**Table V.** Hydrogen coordinates ( $\times 10^4$ ) and isotropic displacement parameters ( $\text{\AA}^2 \times 10^3$ ) for **2**.

	x	y	z	U(eq)
H(2)	770	3209	9705	86
H(3A)	2658	2757	12074	156
H(3B)	3096	2791	10374	156
H(3C)	1688	2447	10797	156
H(5)	-1711	3542	10198	88
H(6)	-3765	3612	11664	90
H(8)	-4916	3494	14175	82
H(10)	-2219	2935	17703	90
H(11)	-179	2841	16203	88
H(13)	926	2934	13657	78
H(14A)	-6436	3762	16266	165
H(14B)	-7148	3320	17232	165
H(14C)	-6682	3203	15573	165
H(16)	2160	7037	7779	72
H(17A)	3913	6902	10588	144
H(17B)	2218	7125	10433	144

H(17C)	3583	7441	9790	144
H(19)	3481	7074	5596	71
H(21)	4814	7150	3180	88
H(22)	6985	7056	1895	92
H(24)	9297	6451	5586	79
H(26)	7910	6349	7990	78
H(27)	5729	6440	9270	74
H(28A)	11407	6714	4167	187
H(28B)	11675	6447	2601	187
H(28C)	10723	6159	3800	187
H(29)	4673	4788	15020	110
H(30)	4881	5722	14656	107
H(31)	3862	5892	11979	88
H(32)	7183	5232	7296	96
H(33)	7222	4301	7810	104
H(34)	4843	4096	9079	89
H(35)	-387	4219	5022	120
H(36)	-306	5160	4505	127
H(37)	906	5567	6750	89
H(38)	-2626	5811	11457	106
H(39)	-2851	4897	12182	94
H(40)	-504	4459	11374	82



H(2N)	3240(50)	4451(8)	12770(50)	108
H(4N)	4740(50)	5552(7)	8340(50)	102
H(6N)	810(60)	4113(11)	7580(60)	134
H(8N)	-280(70)	5873(14)	10100(60)	133

---

**Table VI.** Hydrogen bonds for **2** [ $\text{\AA}$  and  $^\circ$ ].

D-H...A	d(D-H)	d(H...A)	d(D...A)	$\angle$ (DHA)
N(8)-H(8N)...O(5)	0.889(10)	2.14(3)	2.973(8)	155(5)
N(6)-H(6N)...O(1)	0.899(10)	2.32(5)	2.863(5)	119(4)
N(4)-H(4N)...O(4)	0.890(10)	2.04(3)	2.771(4)	138(4)
N(2)-H(2N)...O(2)	0.886(10)	1.81(2)	2.654(5)	158(4)

---

Symmetry transformations used to generate equivalent atoms